Gain-of-function and loss-of-function variants in *GRIA3* lead to distinct neurodevelopmental phenotypes

Berardo Rinaldi,[1,†] Allan Bayat,[2,3,4,†] Linda G. Zachariassen,[2,†] Jia-Hui Sun,[5,6,†] Yu-Han Ge,[5,7] Dan Zhao,[2] Kristine Bonde,[2] Laura H. Madsen,[2] Ilham Abdimunim Ali Awad,[2] Duygu Bagiran,[2] Amal Sbeih,[2] Syeda Maidah Shah,[2] Shaymaa El-Sayed,[2] Signe M. Lyngby,[2] Miriam G. Pedersen,[2] Charlotte Stenum-Berg,[2] Louise Claudia Walker,[8] Ilona Krey,[9] Andrée Delahaye-Duriez,[10,11,12] Lisa T. Emrick,[13,14] Krystal Sully,[13] Chaya N. Murali,[14] Lindsay C. Burrage,[14] Julie Ana Plaud Gonzalez,[13] Mered Parnes,[13,15] Jennifer Friedman,[16,17,18] Bertrand Isidor,[19] Jérémie Lefranc,[20] Sylvia Redon,[21,22] Delphine Heron,[23,24] Cyril Mignot,[23,24] Boris Keren,[25] Mélanie Fradin,[26] Christele Dubourg, [27,28] Sandra Mercier,[29,30] Thomas Besnard,[29,30] Benjamin Cogne, [29,30] Wallid Deb,[29,30] Clotilde Rivier,[31] Donatella Milani,[32] Maria Francesca Bedeschi,[1] Claudia Di Napoli,[1] Federico Grilli,[1] Paola Marchisio,[33,34] Suzanna Koudijs,[35] Danielle Veenma,[35] Emanuela Argilli,[37,38] Sally Ann Lynch,[39] Ping Yee Billie Au,[40] Fernando Eduardo Ayala Valenzuela,[41] Carolyn Brown,[42] Diane Masser-Frye,[43] Marilyn Jones,[44] Leslie Patron Romero,[45] Wenhui Laura Li,[46] Erin Thorpe,[42] Laura Hecher,[46] Jessika Johannsen,[46] Jonas Denecke,[46] Vanda McNiven,[47,48] Anna Szuto,[47,49] Emma Wakeling,[50] Vincent Cruz,[51] Valerie Sency,[51] Heng Wang,[51] Juliette Piard,[52,53] Fanny Kortüm,[54] Theresia Herget,[54] Tatjana Bierhals,[54] Angelo Condell,[55] Bruria Ben Zeev,[56,57] Simranpreet Kaur,[55,58] John Christodoulou,[55,58,59,60] Amelie Piton,[61] Christiane Zweier,[62,63] Cornelia Kraus,[62] Alessia Micalizzi,[64] Marina Trivisano,[65] Nicola Specchio,[65] Gaetan Lesca,[66,67] Rikke S. Møller,[3,4] Zeynep Tümer,[68,69] Maria Musgaard,[8] Benedicte Gerard,[70] Johannes R. Lemke,[71] Yun Stone Shi[5,7,72] and Anders S. Kristensen[2]

[†]These authors contributed equally to this work.

Abstract

AMPA (α-amino-3-hydroxy-5-methyl-4-isoxazole propionic acid) receptors (AMPARs) mediate fast excitatory neurotransmission in the brain. AMPARs form by homo- or heteromeric assembly of subunits encoded by the *GRIA1-GRIA4* genes, of which only *GRIA3* is X-chromosomal.

Increasing numbers of *GRIA3* missense variants are reported in patients with neurodevelopmental disorders (NDD), but only a few have been examined functionally.

Here, we evaluated the impact on AMPAR function of one frameshift and 43 rare missense *GRIA3* variants identified in patients with NDD by electrophysiological assays. Thirty-one variants alter receptor function and show loss-of-function (LoF) or gain-of-function (GoF) properties, whereas 13 appeared neutral.

We collected detailed clinical data from 25 patients (from 23 families) harbouring 17 of these variants. All patients had global developmental impairment, mostly moderate (9/25) or severe (12/25). Twelve patients had seizures, including focal motor (6/12), unknown onset motor (4/12), focal impaired awareness (1/12), (atypical) absence (2/12), myoclonic (5/12), and generalized tonic-clonic (1/12) or atonic (1/12) seizures. The epilepsy syndrome was classified as developmental and epileptic encephalopathy in eight patients, developmental encephalopathy without seizures in 13 patients, and intellectual disability with epilepsy in four patients. Limb muscular hypotonia was reported in 13/25, and hypertonia in 10/25. Movement disorders were reported in 14/25, with hyperekplexia or non-epileptic erratic myoclonus being the most prevalent feature (8/25).

Correlating receptor functional phenotype with clinical features revealed clinical features for *GRIA3*-associated NDDs and distinct NDD phenotypes for LoF and GoF variants. GoF variants were associated with more severe outcomes: patients were younger at the time of seizure onset (median age one month), hypertonic, and more often had movement disorders, including hyperekplexia. Patients with LoF variants were older at the time of seizure onset (median age 16 months), hypotonic, and had sleeping disturbances. LoF and GoF variants were disease-causing in both sexes but affected males often carried *de novo* or hemizygous LoF variants inherited from healthy mothers, whereas all but one affected females had *de novo* heterozygous GoF variants.

Author affiliations:

1 Medical Genetics Unit, Fondazione IRCCS Ca' Granda Ospedale Maggiore Policlinico, Milan, 20122, Italy

2 Department of Drug Design and Pharmacology, University of Copenhagen, Copenhagen, 2100, Denmark

3 Department of Epilepsy Genetics and Personalized Medicine, Danish Epilepsy Centre, Dianalund, 4293, Denmark

4 Department of Regional Health Research, University of Southern Denmark, Odense, 5230 Denmark

5 State Key Laboratory of Pharmaceutical Biotechnology, Model Animal Research Center, Department of Neurology, Nanjing Drum Tower Hospital, Medical School, Nanjing University, Nanjing, 210032, China

6 Zhejiang Key Laboratory of Organ Development and Regeneration, College of Life and Environmental Sciences, Hangzhou Normal University, Hangzhou, 310030 ,China

7 Ministry of Education Key Laboratory of Model Animal for Disease Study, National Resource Center for Mutant Mice, Jiangsu Key Laboratory of Molecular Medicine, Medical School, Nanjing University, Nanjing, 210032, China

8 Department of Chemistry and Biomolecular Sciences, University of Ottawa, Ottawa, K1H 8M5, Canada

9 Institute of Human Genetics, University of Leipzig Medical Center, Leipzig, 04103, Germany

10 Unité fonctionnelle de médecine génomique et génétique clinique, Hôpital Jean Verdier, Assistance Publique des Hôpitaux de Paris, Bondy, 93140, France

11 NeuroDiderot, UMR 1141, Inserm, Université Paris Cité, Paris, 75019, France

12 UFR SMBH, Université Sorbonne Paris Nord, Bobigny, 93000, France

13 Division of Neurology and Developmental Neurosciences, Department of Pediatrics, Baylor College of Medicine, Texas Children's Hospital, Houston, Texas, 77030, USA

14 Department of Molecular and Human Genetics, Baylor College of Medicine, Houston, Texas, 77030, USA

15 Pediatric Movement Disorders Clinic, Texas Children's Hospital and Baylor College of Medicine, Houston, Texas, 77030, USA

16 Rady Children's Institute for Genomic Medicine, San Diego, California, 92123, USA

17 Department of Neurosciences, University of California San Diego, San Diego, CA 92123, USA

18 Department of Pediatrics, University of California San Diego, San Diego, CA 92123, USA

19 Service de Génétique Médicale, Centre Hospitalier Universitaire de Nantes, Nantes, Pays de la Loire, 44000, France

20 Pediatric Neurophysiology Department, CHU de Brest, Brest, 29200, France

21 Service de Génétique Médicale, CHU de Brest, Brest, 29200, France

22 University of Brest, Inserm, EFS, UMR 1078, GGB, Brest, 29200, France

23 APHP Sorbonne Université, Département de Génétique, Hôpital Armand Trousseau and Groupe Hospitalier Pitié-Salpêtrière, Paris, 75013, France

24 Centre de Référence Déficiences Intellectuelles de Causes Rares, Paris, 75013, France

25 Genetic Department, APHP, Sorbonne Université, Pitié-Salpêtrière Hospital, Paris, 75013, France

26 Service de Génétique Médicale, Hôpital Sud, CHU de Rennes, Rennes, 35200, France

27 Service de Génétique Moléculaire et Génomique, CHU de Rennes, Rennes, 35200, France

28 Université de Rennes, CNRS, Institut de Genetique et Developpement de Rennes, UMR 6290, Rennes, 35200, France

29 Nantes Université, CHU Nantes, Service de Génétique Médicale, Nantes, 44000, France

30 Nantes Université, CHU Nantes, CNRS, INSERM, l'institut du thorax, Nantes, 44000, France

31 Department of Paediatrics, Villefranche-sur-Saône Hospital, Villefranche-sur-Saône , 69655, France

32 Fondazione IRCCS Ca' Granda Ospedale Maggiore Policlinico, Milan, 20122, Italy

33 Fondazione IRCCS Ca' Granda Ospedale Maggiore Policlinico, Pediatria Pneumoinfettivologia, Milan, 20122, Italy

34 University of Milan, Milan, 20122, Italy

35 Department of Neurology, ENCORE, Erasmus Medical Center-Sophia Children's Hospital, Rotterdam, 3015, The Netherlands

36 Department of Pediatrics, ENCORE, Erasmus Medical Center-Sophia Children's Hospital, Rotterdam, 3015, The Netherlands

37 Institute of Human Genetics, University of California, San Francisco, CA 94143, USA

38 Department of Neurology, Weill Institute for Neurosciences, University of California, San Francisco, CA 94143, USA

39 Department of Clinical Genetics Children's Health Ireland Crumlin, Dublin, D12 N512, Ireland

40 Department of Medical Genetics, Alberta Children's Hospital Research Institute, Cumming School of Medicine, University of Calgary, Calgary, AB T2N 4N1, Canada

41 Hospital Angeles Tijuana, Tijuana, 22010, Mexico

42 Illumina Inc, San Diego, California, 92122, USA

43 Division of Genetics, Department of Pediatrics, UC San Diego School of Medicine, Rady Children's Hospital, San Diego, California, 92024, USA

44 Facultad de Medicina y Psicología, Universidad Autónoma de Baja California, Tijuana, 22010, Mexico

45 Breakthrough Genomics Inc, Irvine, California, 92618, USA

46 Department of Pediatrics, University Medical Center Hamburg-Eppendorf, Hamburg, 20215, Germany

47 Division of Clinical and Metabolic Genetics, The Hospital for Sick Children, University of Toronto, Toronto, Ontario, ON M5G 1E8, Canada

48 Fred A Litwin Family Centre in Genetic Medicine, University Health Network and Mount Sinai Hospital, Toronto, Ontario, ON M5G 2C4, Canada

49 Department of Paediatrics, Hospital for Sick Children and University of Toronto, Toronto, ON M5G 1E8, Canada

50 North East Thames Regional Genetics Service, Great Ormond Street Hospital for Children NHS Foundation Trust, London, WC1N 3JH, UK

51 DDC Clinic Center for Special Needs Children, Middlefield, Ohio, 44062, USA

52 Centre de Génétique Humaine, Université de Franche-Comté, CHU, Besançon, 25000, France

53 Unité de recherche en neurosciences intégratives et cognitives EA481, Université de Franche-Comté, Besançon, 25000, France

54 Institute of Human Genetics, University Medical Center Hamburg-Eppendorf, Hamburg, 20251, Germany

55 Brain and Mitochondrial Research Group, Murdoch Children's Research Institute, Melbourne, Victoria, 3052, Australia

56 Pediatric Neurology Institute, Edmond and Lily Safra Children's Hospital, Sheba Medical Center, Tel HaShomer, Ramat Gan, 52621, Israel

57 Sackler School of Medicine, Tel Aviv University, Tel-Aviv, 69978, Israel

58 Department of Paediatrics, Melbourne Medical School, University of Melbourne, Melbourne, Victoria, 3052, Australia

59 Discipline of Genetic Medicine, Sydney Medical School, University of Sydney, Sydney, New South Wales, 2050, Australia

60 Discipline of Child & Adolescent Health, Sydney Medical School, University of Sydney, Sydney, New South Wales, 2050, Australia

61 Hôpitaux Universitaires de Strasbourg, Laboratoire de Diagnostic Génétique, Strasbourg, 67000, France

62 Institute of Human Genetics, Friedrich-Alexander-Universität Erlangen-Nürnberg, Erlangen, 91054, Germany

63 Department of Human Genetics, Inselspital Bern, University of Bern, Bern, 3010, Switzerland

64 Translational Cytogenomics Research Unit, Bambino Gesù Children's Hospital, IRCCS, Rome, 00165, Italy

65 Neurology, Epilepsy and Movement Disorders, Bambino Gesù Children's Hospital, IRCCS, Full Member of European Reference Network EpiCARE, Rome, 00165, Italy

66 Department of Medical Genetics, University Hospital of Lyon and Claude Bernard Lyon I University, Lyon, 69100, France

67 Pathophysiology and Genetics of Neuron and Muscle (PNMG), UCBL, CNRS UMR5261 - INSERM U1315, Lyon, 69100, France

68 Kennedy Center, Department of Clinical Genetics, Copenhagen University Hospital, Rigshospitalet, Copenhagen, Denmark

69 Department of Clinical Medicine, Faculty of Health and Medical Sciences, University of Copenhagen, Copenhagen, 2100, Denmark

70 Laboratoires de diagnostic genetique, Institut de genetique Medicale d'Alsace, Hopitaux Universitaires de Strasbourg, Strasbourg, 67000, France

71 Center for Rare Diseases, University of Leipzig Medical Center, Leipzig, 04103, Germany

72 Guangdong Institute of Intelligence Science and Technology, Zhuhai, 519031, China

Correspondence to: Allan Bayat, MD (clinical data)

Department of Epilepsy Genetics and Personalized Medicine, Danish Epilepsy Centre, Dianalund, Denmark

E-mail: abaya@filadelfia.dk

Correspondence may also be addressed to: Yun Stone Shi, PhD (functional evaluation)

Department of Neurology, Nanjing University, Nanjing, China

E-mail: yunshi@nju.edu.cn

Anders Skov Kristensen, PhD (functional evaluation)

Department of Drug Design and Pharmacology, University of Copenhagen, Copenhagen, Denmark

E-mail: ask@sund.ku.dk

Running title: Evaluation of *GRIA3* variants

Keywords: AMPA receptor; GRIA; GRIA3; clinical biomarker; genotype-phenotype

Abbreviations: agonist binding domain = ABD; α-amino-3-hydroxy-5-methyl-4-isoxazolepropionic acid = AMPA; Dulbecco's modified Eagle's medium = DMEM; glutamate = Glu; ionotropic glutamate receptors = iGluR; kainic acid = KA; neurodevelopment disorders = NDDs; N-terminal domain = NTD; whole exome sequencing = WES; two-electrode voltage-clamp = TEVC; transmembrane domain = TMD; C-terminal domain (CTD)

Correspondence to: Allan Bayat, MD (clinical data)

Department of Epilepsy Genetics and Personalized Medicine, Danish Epilepsy Centre, Dianalund, Denmark

E-mail: abaya@filadelfia.dk

Correspondence may also be addressed to: Yun Stone Shi, PhD (functional evaluation)

Department of Neurology, Nanjing University, Nanjing, China

E-mail: yunshi@nju.edu.cn

Anders Skov Kristensen, PhD (functional evaluation)

Department of Drug Design and Pharmacology, University of Copenhagen, Copenhagen, Denmark

E-mail: ask@sund.ku.dk

Running title: Evaluation of *GRIA3* variants

Keywords: AMPA receptor; GRIA; GRIA3; clinical biomarker; genotype-phenotype

Abbreviations: agonist binding domain = ABD; α-amino-3-hydroxy-5-methyl-4-isoxazolepropionic acid = AMPA; Dulbecco's modified Eagle's medium = DMEM; glutamate = Glu; ionotropic glutamate receptors = iGluR; kainic acid = KA; neurodevelopment disorders = NDDs; N-terminal domain = NTD; whole exome sequencing = WES; two-electrode voltage-clamp = TEVC; transmembrane domain = TMD; C-terminal domain (CTD)

Introduction

AMPARs belong to the ionotropic glutamate receptor (iGluR) superfamily of ligand-gated cation channels[1]. AMPARs are activated by glutamate (Glu) binding, which triggers the transient opening of a central pore leading to a millisecond influx of cations, denoted excitatory postsynaptic current (EPSC) that depolarizes the postsynaptic membrane and promotes neuronal firing[2–4]. AMPAR-mediated EPSCs are essential components in most excitatory glutamatergic signalling pathways, and normal AMPAR function is critical for most brain functions, including learning and memory formation[5–13]. The assembly of GluA1-A4 subunits into homo- or heterotetrameric receptor complexes forms diverse subtypes of AMPARs with distinct properties and expression patterns[14,15]. The GluA1-4 subunit proteins are highly similar and have a modular architecture of two extracellular domains, the *N*-terminal domain (NTD) and the agonist binding domain (ABD), a channel-forming transmembrane domain (TMD), and an intracellular carboxy-terminal domain (CTD) of unknown structure (Fig. 1A). The bilobed ABD of each subunit contains a single site where Glu binding initiates conformational changes that are transmitted via semi-flexible linkers to the channel gate in the TMD. Rare genetic variants in the *GRIA1-4* genes[16–21] may disrupt AMPAR physiology and cause developmental and cognitive impairment, behavioural, and psychiatric comorbidities, seizures, and cerebral malformations[19,22–56]. *GRIA1*, *GRIA2*, and *GRIA4* are autosomal genes, whereas *GRIA3* is located on the X-chromosome. While pathogenic missense variants in *GRIA1*, *GRIA2*, and *GRIA4* appear to arise almost

exclusively *de novo*[23,25,28], pathogenic variants in *GRIA3* may be transmitted from healthy mothers to affected male children, which is observed in several X-linked NDDs[27,30].

Currently, 20 *GRIA3* missense variants are reported in 30 patients, of whom four are female[22,26,27,29–35,38,46–49,55]. Of these variants, nine have been functionally tested, revealing or suggesting loss-of-function (LoF) effects for seven variants detected in fiftheen affected males and in one female[22,29,30,33,35] and gain-of-function (GoF) effects in two variants detected in one female and one male[32,34]. Thus, the phenotypic and genetic landscape in *GRIA3*-related disorders remains ill-defined, lacking genotype-phenotype correlations or clinical biomarkers, particularly in females.

We have therefore systematically interrogated the impact on GluA3-containing AMPAR function of 44 rare inherited or *de novo GRIA3* variants identified in patients with NDD to assess these for pathogenicity and establish LoF or GoF effects for overall receptor signalling function. Also, for 25 patients with pathogenic LoF or GoF variants, we compared the clinical features with the functional outcomes to identify genotype-phenotype correlations and clinical biomarkers that could potentially predict the functional outcome of rare *GRIA3* variants. Our results show that *GRIA3*-related disorders encompass two patient groups with distinct clinical features that correlate with the GoF or LoF effect of the variant on receptor function. Also, our findings expand the general knowledge of the pathogenic contribution of rare genetic alterations in *GRIA3* to NDDs in the human population with diverse manifestations, influencing both the timing of disease onset and main clinical symptoms.

Materials and methods

Materials

Unless otherwise stated, all chemicals were from Sigma-Aldrich (St. Louis, MO). Dulbecco's modified Eagle's medium (DMEM), fetal bovine serum, trypsin, and penicillin-streptomycin were from Invitrogen (Carlsbad, CA). DNA modifying enzymes were from New England Biolabs (Ipswich, MA) except PfuUltra II Fusion HS DNA polymerase (Agilent, Carlsbad, CA). Cyclothiazide (CTZ), kainic acid, and NASPM were from HelloBio (Bristol, UK).

Molecular Biology

GRIA3 (MIM 138248) variants were introduced by site-directed mutagenesis into their corresponding positions in cDNA expression constructs encoding GluA3. Specifically, the plasmid vectors pXOOF and pCAGGS-IRES-EGFP containing cDNA for the unedited GluA3 flip and flop isoforms ($GluA3_i$ and $GluA3_o$, respectively) were used for heterologous expression in HEK293 cells or generation of mRNA for microinjection in *Xenopus laevis* oocytes (XOs). For pCAGGS-IRES-EGFP, cDNA for $GluA3_i$ and $GluA3_o$ were subcloned into the *Nhe*I and *Xho*I restriction sites of the vector. For pXOOF, the cDNA for $GluA3_i$ was subcloned into the *EcoR*I and *Xho*I restriction sites. For co-expression with GluA2, GluA2 was subcloned into the vector pCAGGS-IRES-mCherry. Basepair changes in GluA3 were made by the overlapping PCR method or the QuickChange mutagenesis kit (Stratagene, La Jolla, CA). Genetic changes were verified by Sanger DNA sequencing of the entire GluA3 coding region (GATC Biotech, Constance, Germany). When used as templates for *in vitro* transcription of mRNA, plasmid constructs were linearized downstream of the 3' untranslated region using the restriction enzyme *Nhe*I, column purified using NucleoSpin DNA clean-up kit (Macherey-Nagel, Düren, Germany), and stored at a concentration of 1.0 µg/µL at -20 ˚C until use. cRNA transcription was performed using the ARCA mRNA synthesis kit (NEB, Madison, WI, USA). The resulting mRNA was purified using the NucleoSpin RNA Clean-up kit (Macherey-Nagel), diluted to 0.5 ng/nL, and stored at -80 ˚C until use.

Xenopus laevis oocyte preparation and injection

Defolliculated XOs (stage V to VI) were prepared and injected with mRNA as described previously[57]. The care and use of *Xenopus laevis* animals strictly adhered to a protocol (license 2014−15−0201−00031) approved by the Danish Veterinary and Food Administration. Injected XOs were incubated at 18 °C in Modified Barth's Solution (MBS) containing (in mM) 88 NaCl, 1 KCl, 0.41 $CaCl_2$, 2.4 $NaHCO_3$, 0.33 $Ca(NO_3)_2$, 0.82 $MgSO_4$, 5 Tris (pH 7.4) supplemented with 50 µg/ml gentamicin until use. For expression of homomeric GluA3 receptors, XOs were injected with 10 ng cRNA in a volume of 25 nL per oocyte and incubated for 3 days at 18 °C in

MBS until the experiment. For expression of heteromeric GluA2/A3 receptors, injection of 10 ng of a 2:1 mix ratio of GluA2/GluA3 cRNA was used.

HEK293 cell culturing and transfection

HEK293T cells were cultured in a 37 ℃ incubator with 5% CO_2. Transfection was performed in 35-mm dishes using Lipofectamine2000 reagents (Invitrogen). For co-expression of GluA3 and GluA2, the ratio of GluA3 to GluA2 cDNA was 1:1. The competitive antagonist NBQX (100 μM) was included in culture media to block receptor-induced cytotoxicity. Twenty-four hours post-transfection, cells were dissociated with 0.05% trypsin, plated on coverslips pre-treated with poly-D-lysine, and used for experiments 4 h after plating.

Electrophysiology

Two-electrode voltage-clamp (TEVC) electrophysiology in XOs: Glass micropipettes (0.69 mm ID/1.2 mm OD, Harvard Apparatus, Holliston, MA) were pulled on a Sutter P-1000 micropipette puller (Sutter Instruments, Novato, CA) to a tip resistance of 0.5-2.5 MΩ and filled with 3 M KCl. Oocytes were clamped using a two-electrode voltage-clamp amplifier (OC-725C, Warner Instruments, Hamden, CT) and continuously perfused with Frog Ringer's solution containing 115 mM NaCl, 2 mM KCl, 5 mM HEPES, and 1.8 mM $BaCl_2$ (pH 7.6) by gravity-assisted perfusion at flow rates of 2 to 4 mL/min into a vertical oocyte flow chamber. Compounds were dissolved in Frog Ringer's solution and added by bath application. Concentration-response data were recorded at holding potentials in the -40 to -80 mV range. Each compound solution was applied for 10 to 60 s depending on the time needed to obtain steady-state currents. Current signals were low-pass filtered at 5 Hz using an USBPGF-S1 programmable instrumentation low-pass filter (Alliagator Technologies, Cosa Meda, CA) and digitized with a sampling frequency of 10 Hz using a CED 1401plus analog-digital converter (Cambridge Electronic Design, Cambridge, UK) interfaced with a PC running WinWCP software (available from Strathclyde Electrophysiology Software, University of Strathclyde, Glasgow, UK). Concentration-response experiments were performed by measuring agonist-evoked current during stepwise application of increasing concentrations of agonist, as illustrated in Fig. 3E. All experiments were performed at room

temperature. *Whole-cell voltage-clamp electrophysiology in HEK293 cells:* The deactivation and desensitization kinetics of glutamate-evoked currents from WT and mutant GluA3 and GluA2/3 receptors were determined in the whole-cell configuration in HEK293 cells. After the formation of whole-cell configuration, individual HEK293 cells were lifted with 3 to 5 MΩ borosilicate glass pipettes filled with the following internal solution: 135 mM KF, 33 mM KOH, 2 mM $MgCl_2$, 1 mM $CaCl_2$, 11 mM EGTA, 10 mM HEPES (pH 7.2). Glu (10 mM) was dissolved in the extracellular solution: 140 mM NaCl, 2.5 mM KCl, 2 mM $CaCl_2$, 1 mM $MgCl_2$, 10 mM HEPES, 5 mM Glucose (pH 7.2). Glutamate pulses of 1 or 500 ms were applied to cells using a theta-glass pipette mounted on a piezoelectric bimorph driven by gravity. Glutamate-induced currents were recorded using a MultiClamp 700B amplifier (Axon Instruments) with membrane potential held at -70 mV. Current signals were recorded with an Axon Digidata 1440 data acquisition system and with a sampling frequency of 100 kHz following low-pass filtration over 2 kHz. All experiments were performed at room temperature.

Cohort

Patients with inherited or *de novo GRIA3* variants were recruited through an international collaboration with epilepsy and NDD research groups, the Leipzig GRI-registry (https://www.uniklinikum-leipzig.de/einrichtungen/humangenetik/Seiten/GRI-registry.aspx), Decipher[58], ClinVar[59], and via GeneMatcher[60]. We also contacted the healthcare providers of previously published patients to collect new or updated clinical information or used that previously reported in the literature [26,29,33,34,61] (seven patients). Clinical information was collected by the local physicians or caregivers and included data on the age of seizure onset and offset, seizure semiology, developmental trajectory, medical history, physical examination, EEG, and neuroimaging. The study was conducted in agreement with the Declaration of Helsinki. The Leipzig GRI-registry was approved by the local ethical committee; Leipzig/Germany (224/16-ek and 379/21-ek). Since all probands were minors or had cognitive impairment, their parents or legal guardians provided written informed consent.

Data and statistical analysis

Data for concentration-response curves were obtained from analysis of electrophysiological recordings of agonist-evoked current responses using ClampFit 10 software (Molecular Devices, San Jose, CA). Current responses were normalized to the current response by maximal agonist concentration and used to construct composite concentration-response plots from at least 8 oocytes and fitted using GraphPad Prism v9 (GraphPad Software, San Diego, CA, USA) to a four-variable Hill equation:

$$response = bottom + \frac{top - bottom}{1+10^{(logEC50 - X)\times nH}} \quad \text{(Equation 1)}$$

where *bottom* is the fitted minimum response, *top* is the fitted maximum response, *nH* is the Hill slope, *X* is the agonist concentration, and EC_{50} is the half-maximally effective agonist concentration, respectively. The time constants for the rate of desensitization (τ_{desens}) and deactivation (τ_{deact}) were obtained by fitting current responses evoked by 500 and 1 ms Glu pulses with an exponential function using a non-linear least square algorithm (ClampFit):

$$I = I1 \times (\exp\left(-\frac{time}{\tau 1}\right) + I2 \times \left(exp\left(-\frac{time}{\tau 2}\right)\right) \quad \text{(equation 2)}$$

, where I is the total current amplitude, and $I1$ and $I2$ are the amplitudes of the fast and slow current components, respectively, and $\tau 1$ and $\tau 2$ are the time constants for the decay of the fast and slow current components. The weighted average τ was then calculated as follows:

$$\tau_{\text{weighted}} = (\frac{I1 \times \tau 1 + I2 \times \tau 2}{I1 + I2}) \quad \text{(equation 3)}$$

All desensitization time constants were determined using the two-component fitting, and τ_{desens} is reported as the weighted average τ. Except otherwise stated, all deactivation time constants were determined using mono-exponential fitting, using equation 2 with $I2$ fixed at 0. Statistical analyses of data were performed in GraphPad Prism 9. Unless otherwise stated, summary patch-clamp and TEVC electrophysiology data are represented as mean with a 95% confidence interval (CI). One-way analysis of variance (ANOVA) with Dunnett's post hoc multiple comparison test was performed for comparisons of three or more groups in which the data were normally

distributed and where a *P*-value <0.05 was considered significant. For statistical analysis of clinical data, quantitative statistics were analyzed using SPSS software (version 24, IBM, United Kingdom). Two-sided T-test was used to determine the association of clinical features with the LoF and GoF patient groups. *P*-value < 0.05 was considered significant. Unless otherwise stated, the level of statistical significance is denoted as $*P < 0.05$, $**P < 0.01$, and $***P < 0.001$. Extended statistical information including specific *P*-values are provided in the Supplementary information.

Results

GRIA3 missense variants in NDD patients concentrate on domains responsible for glutamate binding and channel gating

To investigate the pathogenicity of *GRIA3* variants identified in NDD patients, we collected one frameshift variant and 43 *GRIA3* missense variants identified in patients with presumed *GRIA3*-related NDD (*Materials and methods*) (Fig. 1, Supplementary table S1). Notably, although the central elements for channel function (the ABD, TMD, and ABD-TMD linkers) constitute less than 50% of the GluA3 subunit protein, the majority of the *GRIA3* missense variants are located in the ABD (15 variants), and TMD (13 variants) domains, and the ABD-TMD linkers (6 variants). In addition, none of these 34/43 variants are reported in the Genome Aggregation Database (gnomAD), and *GRIA3* is predicted to be constrained to missense variants (Z = 4.23), which indicates intolerance to missense variation, and the majority are predicted to be damaging by *in silico* prediction of deleteriousness (Supplementary Table S1). In contrast, only 9 variants affect residues in the NTD and CTD, which are non-critical domains for the core ligand-gated channel function (Fig. 1A) (Supplementary Table S1).

GRIA3 variants have GoF or LoF effects on GluA3 receptor function

The majority of the identified *GRIA3* missense variants have not been functionally evaluated for effects on GluA3-containing AMPAR function, except for variants p.(Arg450Glu), p.(Ala615Val), p.(Arg631Ser), p.(Ala653Thr), p.(Arg660Thr), p.(Met706Thr), p.(Glu787Gly),

p.(Glu787Lys), p.(Gly826Asp), and p.(Gly833Arg)[22,29,30,32–35], although not in a systematic manner. Therefore, we first evaluated all variants with TEVC electrophysiology to directly compare effects, focusing on key receptor functional features that included current amplitude, Glu sensitivity, receptor activation, and desensitization properties (Fig. 1B-C). Specifically, *GRIA3* variants were introduced in cDNA encoding GluA3 and expressed in XOs as homomeric receptors (*Materials and methods*). We first recorded current responses following the application of a single high Glu concentration (300 µM) with pharmacological blockade of receptor desensitization (Fig. 1C). Twenty of the variants showed currents that were significantly lower than WT, including nine variants with undetectable or very small (*e.g.*, 50-fold lower than WT) current amplitude (Fig. 1B-C; Supplementary Table S2), indicating that these variants have severe LoF effects on GluA3 subunit function or expression. The single frameshift variant p.(Gln371Argfs*6) is located in the 5' end of the NTD-encoding segment of the *GRIA3* coding sequence (Fig. 1A). Therefore, this variant results in the expression of only the NTD that cannot form a functional receptor. Indeed, the expression of p.(Gln371Argfs*6) in XOs did not yield any current response (Fig. 1C) and is assigned a complete LoF status. The remaining variants produced current responses with amplitudes similar to or within two-fold range of WT (Fig. 1B and C; Supplementary Table S2), except for the variants p.(Ala615Val), p.(Ser663Pro), and p.(Gly803Glu), which showed more than two-fold significantly increased currents compared to WT, suggesting an overall GoF effect on receptor function.

For all functional variants, we performed dose-response experiments with increasing concentrations of Glu (Fig. 1D), and determined the half-maximally effective concentration (EC_{50}) for receptor activation (Fig. 1E; Supplementary Fig. S2 and Table S3). As summarized in Fig. 1B, 20 variants changed the EC_{50} significantly by more than two-fold. The most pronounced changes were observed for the p.(Ser531Cys), p.(Ala654Thr), p.(Trp799Leu), and p.(Gly803Ala) variants, which decreased EC_{50} more than 20-fold (considered a GoF effect), and p.(Met617Thr) and p.(Phe655Ser), which increased EC_{50} by more than 20-fold (considered a LoF effect; Fig. 1B and E, Supplementary Fig. S2, and Table S3).

AMPARs undergo profound desensitization in the continued presence of Glu, which is a key property for EPSC shape and protects against excitotoxicity due to glutamatergic hyperfunction[62–64]. For variants with a residual function, we assessed potential effects on receptor desensitization by recording consecutive Glu currents in the absence (I_{GLU}) and presence

($I_{GLU+CTZ}$) of CTZ block of desensitization (Fig. 2A). The WT GluA3 receptor showed desensitized current amplitude of 2.8 ± 0.4%, *n* = 79, of the non-desensitized current amplitude (Fig. 2A-B; Supplementary Table S3); corresponding well with previously reported ratios for homomeric GluA3[65–67]. Eight variants displayed significant increases in the desensitized current as illustrated for a representative variant (p.(Ala654Val)) in Fig. 2A. The variants p.(Arg631Ser), p.(Ala654Pro), p.(Ala654Val), and p.(Ala654Thr) showed the most profound effects, with near identical current amplitudes under desensitizing and non-desensitizing conditions (Fig. 2A-B; Supplementary Table S3), which indicate that the variants decrease or fully block receptor desensitization, which is a GoF effect for AMPAR signalling. In contrast, seven variants (p.(Ser531Cys, p.(Leu774Ser), p.(Thr776Met), p.(Trp799Leu), p.(Gly803Ala), p.(Thr816Ile), p.(Gly826Asp)) significantly decreased the desensitized current relative to the non-desensitized current, indicating an increase in receptor desensitization, which is considered a LoF effect (Fig. 2B; Supplementary Table S3).

We screened for changes in the activation properties of GluA3, comparing the receptor current evoked by application of the weak partial agonist kainic acid (KA) versus the current evoked by Glu[68,69] (Fig. 2C). When desensitization was blocked, the KA current (I_{KA+CTZ}) at WT GluA3 was 21 ± 0.1%, *n* = 85, of the Glu current (Fig. 2B; Supplementary Table S3). The results from the screening showed an increased KA efficacy for 12 variants (p. (Ala615Val), p.(Arg631Ser), p.(Ser647Phe), p.(Ala654Prol), p.(Ala654Val), p.(Ala654Thr), p.(Arg660Ser), p.(Arg660Thr), p.(Ser663Pro), p.(Trp799Leu), p.(Gly803Glu), and p.(Gly803Ala) (Fig. 2C; Supplementary Table S3). This effect indicates an increase in the ability of GluA3 to translate agonist binding to channel opening and is to be considered a GoF effect for overall receptor function. In contrast, six variants (p.(Met617Thr), p.(Ala653Thr), p.(Phe655Ser), p.(Ile665Thr), p.(Lys701Glu), and p.(Gly826Asp)) displayed decreased KA efficacy, and, therefore, reduced ability to activate, which is a LoF effect for overall receptor function (Fig. 2B-C; Supplementary Table S3). Notably, the KA/Glu current ratio has previously been electrophysiologically characterized for homomeric GluA3 with the p.(Ala653Thr) variant with similar results[29].

Lastly, we screened for constitutive receptor activity, e.g., channel opening in the absence of Glu, using 1-naphthyl acetyl spermine (NASPM), a selective open-channel blocker for GluA2-lacking calcium-permeable AMPARs[70,71]. Applying 1 µM NASPM produced near-complete inhibition of the Glu-evoked current for WT GluA3 and most variants (Fig. 2C-D;

Supplementary Table S3). However, for two variants (p.(Arg631Ser) and p.(Ala654Pro)), NASPM application inhibited the membrane current below the level observed in the absence of Glu (Fig. 2C), indicating constitutive channel activity. This effect was most profound for the variant p.(Ala654Pro) (Fig. 2D; Supplementary Table S3). Specifically, in the absence of an agonist and at a holding potential of -40 mV, XOs expressing the p.(Ala654Pro) variant displayed approximately 10-fold increased membrane current (564 ± 123 nA; n = 21) compared to XOs expressing the WT (receptor 61 ± 32 nA; n = 20). Also, the elevated membrane current for p.(Ala654Pro) increased relatively little upon Glu application in the presence of block of desensitization ($I_{GLU+CTZ}$ = 89 ± 20 nA; n = 18) compared to the membrane current in WT expressing ($I_{GLU+CTZ}$ = 4230 ± 490 nA; n = 140), but decreased by more than 300% upon NASPM application (Fig. 2D; Supplementary Table S3). Three variants (p.(Ala615Val), p.(Met617Thr), and p.(Gly826Asp) showed decreased inhibition by NASPM. These variants change residues located close to the NASPM binding site in the channel, and the decreased inhibition by NASPM likely reflects a direct effect on the binding affinity of NASPM[72].

The TEVC functional characterizations of the 43 missense *GRIA3* variants showed that 70% (30/43) changed one or more of the evaluated receptor parameters. As summarized in Fig. 2E, 18 of the missense variants showed a pattern of functional effects that point to an overall LoF effect on receptor signalling function, including decreased or complete loss of desensitized and non-desensitized current response to Glu (no or decreased I_{GLU} or $I_{GLU+CTZ}$, respectively), reduced agonist sensitivity (increased EC_{50}), reduced activation ability (decreased I_{KA}/I_{GLU} ratio), or increased desensitization (decreased $I_{GLU}/I_{GLU+CTZ}$ ratio). In contrast, 12 variants showed effect patterns that suggest an overall GoF effect; *e.g.*, increased current amplitudes, agonist sensitivity, activation, including constitutive activity, and significantly reduced or completely blocked desensitization (Fig. 2F). Two variants (p.(Trp799Leu) and p.(Ser531Cys)) showed a mixed pattern of both GoF and LoF effects. Specifically, these variants showed no (p.(Ser531Cys)) or greatly reduced (p.(Trp799Leu)) desensitized current, but WT-like current amplitude upon block of desensitization (Fig. 1B-C, Supplementary Table S2 and S3). These results suggest a LoF functional phenotype due to increased desensitization. On the other hand, both variants decreased Glu EC_{50} dramatically (Fig. 1E; measured in the presence of CTZ), which is a GoF effect, and for p.(Trp799Leu) also increased the KA efficacy, indicating increased ability to be activated (Fig. 1B, Supplementary Table S3). However, we classified both variants to have an overall LoF

effect based on the reduced Glu current without blocked desensitization. Lastly, 13 variants did not show significant changes in any of the evaluated functional parameters (Fig. 2G) and, therefore, appeared neutral for the core ligand-gated channel function and were not investigated further. However, we cannot rule out that these variants may affect other aspects of GluA3-containing receptors beyond the functions studied here, such as receptor trafficking, regulation, and interactions with synaptic proteins important for native AMPARs.

The domain distribution of the GoF, LoF, and functionally neutral variants shows that GoF and LoF variants exclusively affect residues in the ABD, TMD, and ABD-TMD linkers, whereas most neutral variants affect residues in the NTD and CTD (Fig. 2E-G). Overall, the positions in the GluA3 sequence that are affected by LoF and GoF variants fit well with analysis of missense tolerance ratio[73] (MTR) (Fig. 2H), as 87% (27/31) of the variants with functional LoF or GoF affect residues in segments that appear highly intolerant to missense variation (Fig. 2H), whereas 69% (9/13) of the functionally neutral variants affect positions with no unusual sensitivity to missense variation. This observation suggests that MTR analysis is a highly effective predictor of potential pathogenicity of missense variants for *GRIA3*. In comparison, the accuracy of the *in silico* prediction tools SIFT and PolyPhen in predicting the LoF/GoF variants as pathogenic was 72% and 74%, respectively (Supplementary Table S1).

GRIA3 variant effects are dominant in heteromeric AMPA receptors

GluA3 subunits are thought to preferentially assemble with GluA2 subunits into heteromeric GluA2/3 receptors in the brain, although triheteromeric GluA1/2/3 receptors have also recently been shown[74–77]. Thus, native GluA3-containing AMPARs in affected patients will have two subunits containing the variant. To assess whether variant effects were also present in heteromeric GluA2/A3 receptors, we expressed the LoF or GoF variants together with WT GluA2 and determined desensitized and non-desensitized current amplitudes, the degree of desensitization, and the KA/GLU response ratio (Fig. 3A-C; Supplementary Table S4). For each variant expressed with GluA2, the current-voltage (IV) relationship was determined, as this provides a measure for formation of heteromeric GluA2/A3 receptors (Fig. 3E). Specifically,

incorporation of GluA2 subunits shifts the IV curve from inwardly-rectifying to linear (as illustrated for WT and selected variants in Fig. 3E). All functional variants exhibited linear IV relationships when expressed with GluA2, which shows that the variants retain their ability of GluA3 to form heteromeric GluA2/A3 receptors. As summarized in Fig. 3D, the results showed that GoF effects observed in homomeric GluA3 were highly penetrant to heteromeric GluA2/A3. Specifically, significant changes for the affected parameters were also observed in GluA2/A3 receptors for all variants exhibiting one or more GoF effects. Similarly, for variants that induced a LoF phenotype for homomeric GluA3, LoF effects were also observed in the heteromeric receptor background. Notably, among the variants that completely abolished the Glu response in homomeric GluA3 (p.(Gly492Ser), p.(Gly630Arg), p.(Met706Thr), p.(Gly721Arg), p.(Glu787Lys), p.(Glu787Gly), and p.(Gly833Arg)), currents could be measured for all when expressed as heteromers with GluA2, although with profoundly lower current amplitudes than WT GluA2/A3 (Fig. 3D, Supplementary Table S2). The only exception was the p.(Gly721Arg) variant, which showed a current amplitude similar to WT in heteromeric GluA2/A3 receptors (Supplementary Table S2). For all of these variants, a linear IV relationship similar to WT GluA2/3 was observed (Supplementary Fig. S3), confirming the presence of the GluA2 subunit in the heteromeric receptor complex.

In summary, the characterization of the effects of the 43 *GRIA3* missense variants revealed 31 (72%) to alter electrophysiological functions in both homomeric GluA3 and heteromeric GluA2/3 receptors, strongly indicating these variants as pathogenic.

Kinetic characterization and classification of the pathogenic variants

Based on the TEVC evaluations, we next aimed to collect detailed phenotypic and genetic information from patients carrying the 31 *GRIA3* variants associated with significant LoF or GoF effects on receptor function and, therefore, are strongly indicated as a monogenetic cause of NDD. For 17 of these variants, we obtained detailed clinical information from 25 NDD patients, resulting in a cohort of 14 males (patients M1-M14) and 11 females (patients F1-F11). The genetic and phenotypic details of the patient cohort are described in the Supplementary results

and Supplementary Table S7. To further characterize how the 17 cohort variants perturb the receptor functional phenotype, we utilized fast-application patch-clamp electrophysiology, which can model the synaptic Glu pulses that evoke EPSCs on a millisecond timescale and can accurately identify changes in receptor deactivation and desensitization rates that are particularly important for shaping AMPAR synaptic signals. Specifically, the cohort variants were expressed in HEK293 cells as homomeric GluA3 and heteromeric GluA2/A3 receptors. Current responses to pulses of 10 mM Glu were recorded (*Materials & Methods*) (see Fig. 4A for an illustration of the recording protocol and representative current traces), except for variants p.(Ala653Thr), p.(Gly630Arg), and p.(Arg660Thr), which have previously been characterized with fast-application patch-clamp electrophysiology in both homomeric GluA3 and heteromeric GluA2/A3 receptors[29,34,61]. AMPAR subunits occur in two isoforms, denoted flip and flop, which result from alternative splicing of the two mutually exclusive exons, 14 and 15, respectively, and have important differences in receptor kinetics[78]. This alternative flip/flop splicing affects nine amino acid positions in a 38 amino acid segment close to the ABD-M4 linker. The p.(Glu787Gly) (patient M7), p.(Glu787Lys) (patient M8-9, F11), and p.(Trp799Leu) (patient F9) variants originate in exon 14 and specifically affect the flop isoform. Therefore, these variants were characterized in the flop isoform of GluA3 ($GluA3_o$). The remaining variants are located outside the flip/flop segment and were characterized in the flip isoform ($GluA3_i$), which predominates before birth and continues to be expressed in the adult brain[79].

The results showed a complete or very severe LoF effect on the current response to fast Glu applications for the variants p.(Gly492Ser) (patient M2), p.(Phe655Ser) (patient M10), p.(Ile665Thr) (patient F10), and p.(Glu787Gly) (patient M7) (Fig. 4A). In addition, the variants p.(Gly630Arg) (patients M3-6) and p.(Glu787Lys) (patient M8-9, F11) that previously have been characterized with identical recording protocols, also have a complete LoF phenotype[61]. Moreover, expressed together with WT GluA2, all these variants also abolished the current response in heteromeric GluA2/A3 receptors, except for p.(Ile665Thr) (patient F10), which showed a robust and desensitizing current response (Fig. 4A). To test whether the complete or severe LoF effect was due to the variants perturbing expression and folding of the GluA3 subunit protein, or subunit ability to assemble into receptors that traffic to the membrane, we expressed β-lac-tagged WT and variant GluA3 constructs in HEK293 cells (Supplementary methods). Analysis of the conversion rates of the β-lac substrate nitrocefin from transfected HEK293 cells

revealed no significant difference in cell-surface expression between WT and variant receptors (Supplementary Fig. S4). Thus, we conclude that the LoF effect that these variants have on Glu current is due to disruption of the core ligand-gated channel function of the receptor. The p.(Trp799Leu) variant showed measurable currents but with greatly reduced peak amplitude. In homomeric GluA3, due to the reduced currents we were only able to reliably determine the desensitization rate of the p.(Trp799Leu) variant in a single experiment, which showed 3-fold increased rate of desensitization (τ_{des} = 0.57 ms versus 1.58 ± 0.05 ms; n = 15 for WT $GluA3_o$) and no measurable steady-state current (Fig. 4A-B; Supplementary table S5). These effects were also observed in the heteromeric GluA2/A3 receptor (Fig. 4A-B; Supplementary table S5), where slightly more robust currents allowed us to accurately determine the desensitization kinetics. and suggest p.(Trp799Leu) is a severe LoF variant by greatly reducing charge transfer due to an increased rate and extent of receptor desensitization. Notably, this is supported by the TEVC characterizations that showed that the diminished Glu current for p.(Trp799Leu) could be fully rescued by the pharmacological block of desensitization (Fig. 2 and 3).

The GoF variants p.(Ala654Val), p.(Ala654Thr), p.(Ala654Pro), p.(Ser663Pro), p.(Lys701Glu), p.(Gly803Ala), and p.(Gly803Glu) all produced robust currents when expressed as homomeric and heteromeric receptors (Fig. 4A). For these variants we determined the desensitization rate (τ_{des}) and peak-to-steady-state current ratio (I_{ss}) from 500 ms glutamate stimulations (Fig. 4B-C) and the deactivation rate (τ_{deact}) from 1 ms stimulations (Fig. 4D-E, Supplementary table S5) (Materials and methods). As predicted from the TEVC results, p.(Ala654Val) (patient F5), p.(Ala654Thr) (patient F7), and p.(Ala654Pro) (patient F6) displayed greatly decreased desensitization. Specifically, whereas WT $GluA3_i$ currents almost completely decayed within milliseconds (τ_{des} = 5.3 $\pm$ 0.3 ms; n = 12) to a small fraction of the peak current (I_{ss} = 1.1 $\pm$ 0.1%; n = 16), the p.(Ala654Pro) variant completely blocked (I_{ss} = 100 ± 0.0%, n = 4), and the p.(Ala654Thr) and p.(Ala654Val) variants greatly reduced the level of desensitization (I_{ss} = 82 $\pm$ 3%, n = 9, and 61 $\pm$ 2%, n = 9, respectively). In addition, the deactivation rates for these variants were also slowed (τ_{deact} = 5-22 ms; n = 3-9) compared to WT (τ_{deact} = 2.1 $\pm$ 0.2 ms; n = 9) for homomeric GluA3 receptors (Fig. D-E, Supplementary table S5). These effects were maintained for the heteromeric GluA2/A3 receptor, where the p.(Ala654Pro) variant completely blocked desensitization and slowed deactivation, and the p.(Ala654Val) and p.(Ala654Thr) decreased desensitization and slowed deactivation, except for p.(Ala654Val),

which showed a deactivation rate not different from WT (Fig. B-C, Supplementary table S5). Thus, the three variants affecting Ala654 can be classified as severe GoF due to profoundly decreased desensitization and reduced deactivation rates. The variants p.(Ser663Pro) (patient F4) and p.(Lys701Glu) (patient F3) displayed phenotypes quite similar to each other, which included significantly increased I_{ss} levels, slowed desensitization rates, and modestly but significantly slowed deactivation rates in both homomeric and heteromeric receptors (Fig. B-C, Supplementary table S5). Lastly, the two variants affecting Gly803 (p.(Gly803Ala) and p.(Gly803Glu)) showed normal I_{ss} levels but reduced desensitization and deactivation rates (Fig. B-C, Supplementary Table S5). These changes, as a consequence of p.(Ser663Pro), p.(Lys701Glu), p.(Gly803Ala), and p.(Gly803Glu) variants, are predicted to have a clear GoF effect on the synaptic charge carried by GluA3-containing AMPARs, although to a less severe extent than the variants affecting Ala654.

Correlation of LoF and GoF receptor effects with patient clinical phenotype

We next compared patient clinical information with the receptor phenotypic information. As summarized in Fig. 5A, we classified the variants based on the GoF and LoF effects identified in the electrophysiological analyses as severe or mild. In addition, data from previously reported evaluations of the p.(Ala653Thr)[29] and p.(Arg660Thr)[34] variants were included. For LoF variants, the severe class includes seven variants in 11 patients (M1-M10 and -F10; Fig. 5A) that completely abolish the current response to millisecond Glu stimulation, whereas the mild class includes two variants from three patients (p.(Ala653Thr) in patients M11-12 and p.(Trp799Leu) in patient F9), which show current response to fast Glu stimulation, but with greatly reduced amplitude and profound changes in desensitization and deactivation kinetics that overall are predicted to reduce synaptic charge transfer. For GoF variants, the mild class includes four patients with variants p.(Gly803Ala) (patient M13) and p.(Gly803Glu) (patients M14 and F1-2), which slow desensitization and deactivation rates significantly and increase Glu sensitivity, but do not appear to change peak or desensitized current levels. The severe GoF class includes the variants p.(Ala654Val), p.(Ala654Pro), and p.(Ala654Thr) (patients F5-F7), respectively)), in addition to p.(Ser663Pro) (patient F4)), p.(Arg660Thr) (patient F8)), and p.(Lys701Glu) (patient

F3), which all significantly reduce desensitization and deactivation rates, increase Glu sensitivity and increase steady-state current amplitudes in the TEVC experiments (Fig. 5A).

Several differences between the GoF and LoF patient classes (10 patients with GoF variants and 15 patients with LoF variants) were identified (Table 1 and Fig. 5B). Importantly, LoF and GoF variants are disease-causing in both sexes but affected males predominantly (12/14) carry hemizygous LoF variants. In contrast, most affected females (8/11) carry heterozygous GoF variants. Another striking difference includes the age of seizure onset in the subgroup of patients with epileptic comorbidities, muscle tone (hypo- versus hypertonia), sleep difficulties, and movement disorders, including hyperekplexia (Fig. 5B and Table 1). Specifically, for the patients with epileptic comorbidities, the median age of seizure onset in patients harboring a GoF was 1 month (range 1st day-12 months, $n = 5$), being significantly earlier than in patients with LoF variants, being 16.5 months (range 12-36 months, $n = 6$, $P = 0.004$). We detected no significant differences between the GoF and LoF groups when comparing seizure types ($P = 0.85$) and treatment response ($P = 1$). For body tone, most patients harboring a LoF variant had congenital muscular hypotonia ($n = 10/15$), which was not reported in any of the 10 patients with GoF variants ($P = 0.0004$). In contrast, congenital muscular hypertonia was present in 8/10 patients with GoF variants, while it was only reported in 1/15 patients with LoF variants ($p = 0.0002$). Sleep disturbances were reported in 10/15 patients with LoF variants, while they were only present in 2/10 patients with GoF variants ($p = 0.0018$). Movement disorders of any kind were reported in 5/15 patients with LoF variants, while they were present in 8/10 patients with a GoF variant ($p = 0.04$). In particular, an excessive startle response to external stimuli, also known as hyperekplexia, was more prevalent in the group with GoF variants ($n = 5$) compared to the group with LoF variants ($n = 1$) ($p = 0.003$). For behavioural abnormalities, aggressive outbursts were more prevalent in the LoF cohort ($n = 6$) compared to the GoF cohort ($n = 2$), although the difference was not significant ($p = 0.29$). There were no significant differences in the other behavioural abnormalities reported in the GoF ($n = 6$) compared to the LoF cohort ($n = 10$) ($p = 0.75$). Although all patients had ID, we found no significant difference in severity between the GoF and LoF cohorts ($p = 0.26$). Specifically, ID was reported to be borderline/mildly ($n = 1$), moderately ($n = 5$), severely ($n = 8$), or profoundly ($n = 1$) affected in the LoF cohort, while moderately ($n = 4$), severely ($n = 3$) or profoundly ($n = 3$) affected in the GoF cohort.

In summary, the phenotypic assessment indicates that GoF variants are objectively associated with more severe outcomes: patients were younger at the time of seizure onset, hypertonic, and more often had movement disorders, including hyperekplexia. In contrast, patients with LoF variants were older at seizure onset, hypotonic, and had sleep difficulties.

Discussion

Missense variants in *GRIA3* are by far the most prevalently reported *GRIA* genetic defects in NDD patients. However, the extent to which the variants underlie NDDs is not clear, as few have been studied in cellular or animal models to confirm them as pathogenic variations. The present work systematically evaluates 44 rare *GRIA3* variants in NDD patients to establish whether these have functional effects on GluA3-containing AMPARs. Focusing on effects on core ligand-gated ion channel function, we find that 31 variants produced significant effects and were classified as LoF or GoF concerning overall receptor signalling capability. We correlate the identified effects on receptor function with the clinical features and find distinct GoF and LoF phenotypes. This specific LoF-GoF difference in clinical phenotype is in line with several other central nervous system (CNS) ion channel gene families, including the *GRIN* iGluR gene subfamily[80], where studies applying detailed electrophysiological analysis of rare missense variant effects have established both LoF and GoF effects as pathogenic, with each category often leading to different disease phenotypes[81–86]. In addition to the clinical importance of providing a diagnosis and new disease understanding, identifying pathogenic variants as having LoF or GoF effects on channel function is also of therapeutic relevance as it potentially guides pharmacological intervention. For the iGluR gene families, this approach of systematic and detailed testing of pathogenic variants from patient cohorts and their clinical and therapeutic relevance has been successfully implemented for the NMDAR-encoding *GRIN* gene family, leading to a definition of specific neurological conditions associated with types of variant effect and examples of successful therapeutic intervention[64,87,88]. In this paper, we extend the value of this approach to the *GRIA* family. Moreover, our data advances the understanding of the role of abnormal function of AMPARs in general and GluA3-containing subtypes in particular in NDD syndromes. Firstly, as 71% of the evaluated variants altered GluA3-containing AMPAR function, *GRIA3* can be firmly classified as a general disease gene in NDDs, and underscores the

importance of appropriate AMPAR signalling for CNS development, as also suggested in single case or smaller cohort studies for *GRIA1*, *GRIA2*, and *GRIA3*[22,29,30,32–34]. Secondly, our work expands the spectrum and frequency of functional effects of pathogenic *GRIA3* variants by identifying distinct types of LoF and GoF effects and providing clear genotype-phenotype correlations that define two clinical phenotypes associated with predicted LoF and GoF effects: LoF variants often lead to muscular hypotonia, hyporeflexia, a sleep disorder, aggressive behaviour and later onset of seizures, whereas GoF variants are associated with muscular hypertonia, hyperreflexia, startle-induced non-epileptic myoclonia and earlier onset of seizures.

Although the GoF variants appear to be associated with more severe outcomes, such as earlier seizure onset and a higher prevalence of movement disorders, including hyperekplexia, all patients present with overall severe NDD phenotypes independent of the type of LoF or GoF effect of the *GRIA3* variants. This observation suggests that even quantitatively small alterations from WT AMPAR function lead to severe outcomes, which likely reflects the crucial role of AMPARs in the ability of excitatory synapses to detect transmission events rapidly. As excitatory synaptic currents can occur at rates of up to several hundred Hz, AMPARs have likely evolved with precisely balanced Glu sensitivity and extremely fast rates of activation, desensitization, and deactivation within a very narrow range. Thus, although some LoF and all GoF effects do not prevent the contribution of GluA3-containing AMPARs to synaptic transmission, they are likely to perturb the fidelity of neuronal activation. It is also noteworthy that patient M1, who is hemizygous for the protein-truncating complete LoF variant p.(Gln371Argfs*6), appears to have the least severe symptoms compared to those with missense LoF variants, in particular in respect to the severity of ID (Table 1). This finding suggests that the complete loss of GluA3-containing receptors from synaptic AMPAR populations is better tolerated than the existence of GluA3-containing receptors with perturbed function. Interestingly, similar findings have been reported for γ-Aminobutyric acid A ($GABA_A$) receptors[89]. Further detailed evaluation of more pathogenic *GRIA3* variants is warranted to explore how clinical severity correlates to variant effects on receptor function and will likely require establishing models for studying the variant impact on synaptic transmission and animal behavioural phenotypes.

The current data set also provides insight into emerging associations among sex and inheritance, which often is complicated for morbid genes on the X-chromosome, as it is not

always possible to predict the phenotypical effect in heterozygous females. Our data set establishes that LoF and GoF variants as disease-causing in both sexes, but that affected males more often (12/14) carry hemizygous LoF variants, whereas most affected females (8/11) carry heterozygous GoF variants. Although our data do not support a strict model, the prevalence of *de novo* GoF in females is consistent with the general understanding that LoF variants are likely to be less harmful in heterozygous females[90]. However, evaluation of further *GRIA3* variants in males and females is needed to explore *i*) the prevalence of GoF variants in females and LoF variants in males and *ii*) to describe if males with GoF variants are equally or more severely affected than females with similar variants.

Next-generation sequencing has become routine in hospitals, and the number of NDD patients with a genetic etiology is increasing[91,92]. As a result, the number of new *GRIA* variants needing a functional assessment is expected to rise. In addition to confirming pathogenicity, functional testing provides knowledge crucial for treatment, as choosing the right drug (effective and not exacerbating the existing symptoms) depends on establishing LoF or GoF status. In this respect, establishing the impact of new variants on AMPAR function via electrophysiological evaluation may become a critical bottleneck in individual cases, highlighting a need to develop approaches for the theoretical prediction of variant pathogenicity and LoF/GoF effects. Notably, recent large-scale bioinformatical efforts for exploring new approaches for prediction of pathogenicity of variants in genes encoding voltage- and ligand-gated ion channel subunits have suggested that clinical decision support algorithms that predict LoF/GoF status based on location in protein structure may become feasible[93]. Specifically, it was shown that certain positional measures of the variant in the structures of voltage-gated sodium channels and NMDA receptors could be correlated to functional effect and clinical phenotype[93]. For similar purpose in GluA3-containing AMPA receptors, we note that when considering the variant distribution throughout the GluA3 structure, it is observed that functionally neutral variants are enriched in the NTD, whereas LoF or GoF variants localize in the ABD, linker, and TMD segments (Fig. 1 and 2). However, we find several examples of close clustering of neutral, LoF, and GoF variants in these domains, which suggests that the clinical interpretation of missense variants in *GRIA3* as well as GoF/LoF classifications based on general localization measures in the receptor structure should be cautious.

For several pathogenic *GRIA3* variants, our analysis allows us to pinpoint the mechanistic cause of the overall LoF or GoF effect. This knowledge provides an opportunity for exploring clinically relevant AMPAR drugs for the pharmacological rescue of receptor function among different classes of variant phenotypes. Notably, for variants with LoF effects on AMPAR kinetics, positive allosteric modulators (PAMs) exist, in particular of the *ampakine* class, that can modulate AMPAR current amplitude and waveform via selective effects on receptor kinetics[94]. Although no AMPAR PAM currently is FDA/EMA approved, several have passed Phase I/II clinical trials, such as CX516[95], CX717 (Fasoracetam)[96], Org 24448 (Aniracetam)[97], and CX1739[98], including early proof-of-concept trials in patients with cognitive impairments[99], and are subjects for ongoing clinical development. Similarly, for variants with GoF effects (e.g., increased activation or decreased desensitization), negative allosteric modulators (NAMs) can be explored, including perampanel, which inhibits activation and accelerates desensitization[100]. Importantly, perampanel is approved for chronic treatment of several types of epilepsy[101], and therefore, directly available as a potential precision medicine for patients with GoF AMPAR mutations, as recently has been demonstrated for GoF variants in other *GRIA* genes[102].

The present study represents the largest functional evaluation of missense variants in any *GRIA* gene. Together with previous work on *GRIA1*, *GRIA2*, and *GRIA3*, the volume of validated pathogenic *GRIA* variants has now reached a critical point that firmly establishes *GRIA* genetic defects as the cause of an emerging neurological disease, recently referred to as *GRIA* disorder[102]. However, further understanding of *GRIA* disorder disease mechanisms and potentially devising standard rescue pharmacological strategies is complicated by the diversity of the native AMPAR subtypes that a pathogenic variant can affect. Notably, we focused our functional work on the homomeric GluA3 and the heteromeric GluA2/A3 subtypes in two heterologous expression models, which lack the postsynaptic proteins that interact with native AMPARs and contribute to their synaptic functions. Most native AMPARs assemble with different transmembrane AMPA receptor regulatory proteins (TARPs), which act as auxiliary subunits and have distinct effects on receptor function, including modulation of receptor gating and desensitization properties[64,103]. These effects may have significant implications for the variant effect on synaptic transmission, and further work is required to provide insights into how *GRIA* variants affect AMPAR function involving auxiliary subunits. Also, the absence of a neuronal environment presents a caveat to the classification of variants that do not display

functional effects, as functionally neutral variants may have detrimental effects on other aspects of AMPAR cellular biology, such as receptor incorporation and positioning at synapses and regulation during synaptic plasticity mechanisms. Specifically, our evaluation did not reveal effects on the core function of GluA3-containing AMPARs for 13 variants when evaluated in recombinant GluA3 receptors (Fig. 1). Recent progress in mapping the AMPAR interactome in the brain shows that native AMPARs during the receptor lifetime interact with more than 40 intracellular, extracellular, or membrane-embedded proteins, which are important for proper receptor biogenesis, postsynaptic positioning, and function[104]. We cannot rule out that apparently neutral variants may indeed influence expression and function of native GluA3-constaining AMPARs by interfering with the ability of the GluA3 subunit to interact with synaptic constituents, and confident classification of *GRIA3* variants as neutral is thus not possible in current practise. Therefore, studies beyond establishing the functional defects of *GRIA* variants are needed to describe effects in a synaptic context. Importantly, the impact of LoF/GoF variants on the AMPAR-component of EPSC currents should be determined and correlated with the effects on kinetic parameters obtained from heterologous expression systems. This will improve the framework of predicting synaptic effects for variants based on functional evaluations in reduced systems such as XOs or HEK293 cells.

We have characterized the consequences of 44 *GRIA3* variants identified in NDD patients on GluA3-containing receptor function. Although the spectrum of variant effects on AMPAR signalling mechanisms that underlie the phenotype of each patient is likely to be complex, our analysis shows two significant genotype-phenotype correlations that correspond to predicted GoF or LoF effects on the signalling function of GluA3-containing AMPARs.

Data availability

The authors confirm that the data supporting the findings of this study are available in the main text and its supplementary material.

Acknowledgements

We thank the families for participating in this study. This study makes use of data generated by the DECIPHER community. A full list of centers that contributed to the generation of the data is available from https://deciphergenomics.org/about/stats and via e-mail from contact@deciphergenomics.org. Funding for the DECIPHER project was provided by Wellcome [grant number WT223718/Z/21/Z]. This work has been generated within the European Reference Network on Rare Congenital Malformations and Rare Intellectual Disability (ERN-ITHACA) [EU Framework Partnership Agreement ID: 3HP-HP-FPA ERN-01-2016/739516]. In addition, we thank the ERN EPICARE network for promoting our collaborative call on *GRIA*-related disorders.

Funding

AB (Allan Bayat) is funded by Novo Nordisk Foundation BRIDGE Programme (NNF20SA0064340). JHS (Jia-Hui Sun) is supported by the National Natural Science Foundation of China (32200779). The research conducted at the Murdoch Children's Research Institute (MCRI) was supported by the Victorian Government's Operational Infrastructure Support Program. The Royal Children's Hospital Foundation generously supports the Chair in Genomic Medicine awarded to JC. LCB (Lindsay Catherine Burrage) is supported by NIH (5U54OD030165). YSS (Yun Stone Shi) is supported by the National Key R & D Program of China (2019YFA0801603), the National Natural Science Foundation of China (32170951), the Fundamental Research Funds for the Central Universities (021414380533) and Special Fund for Science and Technology Innovation Strategy of Guangdong Province (2021B0909050004). ASK (Anders Skov Kristensen) is supported by Independent Research Fund Denmark (3101-00386B).

Competing interests

The authors report no competing interests.

Supplementary material

Supplementary material is available at *Brain* online.

References

1. Hansen KB, Wollmuth LP, Bowie D, et al. Structure, Function, and Pharmacology of Glutamate Receptor Ion Channels. *Pharmacol Rev*. 2021;73(4):298-487. doi:10.1124/pharmrev.120.000131
2. Raman IM, Trussell LO. The kinetics of the response to glutamate and kainate in neurons of the avian cochlear nucleus. *Neuron*. 1992;9(1):173-186. doi:10.1016/0896-6273(92)90232-3
3. Sah P, Hestrin S, Nicoll RA. Properties of excitatory postsynaptic currents recorded in vitro from rat hippocampal interneurones. *J Physiol*. 1990;430:605-616. doi:10.1113/jphysiol.1990.sp018310
4. Silver RA, Traynelis SF, Cull-Candy SG. Rapid-time-course miniature and evoked excitatory currents at cerebellar synapses in situ. *Nature*. 1992;355(6356):163-166. doi:10.1038/355163a0
5. Hayashi Y, Shi SH, Esteban JA, Piccini A, Poncer JC, Malinow R. Driving AMPA Receptors into Synapses by LTP and CaMKII: Requirement for GluR1 and PDZ Domain Interaction. *Science*. 2000;287(5461):2262 LP - 2267. doi:10.1126/science.287.5461.2262
6. Barria A, Muller D, Derkach V, Griffith LC, Soderling TR. Regulatory phosphorylation of AMPA-type glutamate receptors by CaM-KII during long-term potentiation. *Science*. 1997;276(5321):2042-2045. doi:10.1126/science.276.5321.2042
7. Kauer JA, Malenka RC, Nicoll RA. A persistent postsynaptic modification mediates long-term potentiation in the hippocampus. *Neuron*. 1988;1(10):911-917. doi:10.1016/0896-6273(88)90148-1
8. Mahanty NK, Sah P. Calcium-permeable AMPA receptors mediate long-term potentiation in interneurons in the amygdala. *Nature*. 1998;394(6694):683-687. doi:10.1038/29312

9. Rumpel S, LeDoux J, Zador A, Malinow R. Postsynaptic Receptor Trafficking Underlying a Form of Associative Learning. *Science*. 2005;308(5718):83-88. doi:10.1126/science.1103944

10. Lee HK, Takamiya K, Han JS, et al. Phosphorylation of the AMPA Receptor GluR1 Subunit Is Required for Synaptic Plasticity and Retention of Spatial Memory. *Cell*. 2003;112(5):631-643. doi:10.1016/S0092-8674(03)00122-3

11. Esteban JA, Shi SH, Wilson C, Nuriya M, Huganir RL, Malinow R. PKA phosphorylation of AMPA receptor subunits controls synaptic trafficking underlying plasticity. *Nat Neurosci*. 2003;6(2):136-143. doi:10.1038/nn997

12. Hu H, Real E, Takamiya K, et al. Emotion Enhances Learning via Norepinephrine Regulation of AMPA-Receptor Trafficking. *Cell*. 2007;131(1):160-173. doi:10.1016/j.cell.2007.09.017

13. Kessels HW, Malinow R. Synaptic AMPA Receptor Plasticity and Behavior. *Neuron*. 2009;61(3):340-350. doi:10.1016/j.neuron.2009.01.015

14. Schwenk J, Baehrens D, Haupt A, et al. Regional diversity and developmental dynamics of the AMPA-receptor proteome in the mammalian brain. *Neuron*. 2014;84(1):41-54. doi:10.1016/j.neuron.2014.08.044

15. Swanson GT, Kamboj SK, Cull-Candy SG. Single-Channel Properties of Recombinant AMPA Receptors Depend on RNA Editing, Splice Variation, and Subunit Composition. *J Neurosci*. 1997;17(1):58-69. doi:10.1523/JNEUROSCI.17-01-00058.1997

16. Keinänen K, Wisden W, Sommer B, et al. A family of AMPA-selective glutamate receptors. *Science*. 1990;249(4968):556-560. doi:10.1126/science.2166337

17. Puckett C, Gomez CM, Korenberg JR, et al. Molecular cloning and chromosomal localization of one of the human glutamate receptor genes. *Proc Natl Acad Sci U S A*. 1991;88(17):7557-7561. doi:10.1073/pnas.88.17.7557

18. Sun W, Ferrer-Montiel AV, Schinder AF, McPherson JP, Evans GA, Montal M. Molecular cloning, chromosomal mapping, and functional expression of human brain glutamate receptors. *Proc Natl Acad Sci U S A*. 1992;89(4):1443-1447. doi:10.1073/pnas.89.4.1443

19. Gécz J, Barnett S, Liu J, et al. Characterization of the human glutamate receptor subunit 3 gene (GRIA3), a candidate for bipolar disorder and nonspecific X-linked mental retardation. *Genomics*. 1999;62(3):356-368. doi:10.1006/geno.1999.6032

20. Boulter J, Hollmann M, O'Shea-Greenfield A, et al. Molecular cloning and functional expression of glutamate receptor subunit genes. *Science*. 1990;249(4972):1033-1037. doi:10.1126/science.2168579

21. Hollmann M, O'Shea-Greenfield A, Rogers SW, Heinemann S. Cloning by functional expression of a member of the glutamate receptor family. *Nature*. 1989;342(6250):643-648. doi:10.1038/342643a0

22. Piard J, Béreau M, XiangWei W, et al. The GRIA3 c.2477G > A Variant Causes an Exaggerated Startle Reflex, Chorea, and Multifocal Myoclonus. *Mov Disord*. 2020;35(7):1224-1232. doi:10.1002/mds.28058

23. Geisheker MR, Heymann G, Wang T, et al. Hotspots of missense mutation identify neurodevelopmental disorder genes and functional domains. *Nat Neurosci*. 2017;20(8):1043-1051. doi:10.1038/nn.4589

24. Hackmann K, Matko S, Gerlach EM, et al. Partial deletion of GLRB and GRIA2 in a patient with intellectual disability. *Eur J Hum Genet*. 2013;21(1):112-114. doi:10.1038/ejhg.2012.97

25. Salpietro V, Dixon CL, Guo H, et al. AMPA receptor GluA2 subunit defects are a cause of neurodevelopmental disorders. *Nat Commun*. 2019;10(1):3094. doi:10.1038/s41467-019-10910-w

26. Trivisano M, Santarone ME, Micalizzi A, et al. GRIA3 missense mutation is cause of an x-linked developmental and epileptic encephalopathy. *Seizure*. 2020;82:1-6. doi:10.1016/j.seizure.2020.08.032

27. Philips AK, Sirén A, Avela K, et al. X-exome sequencing in Finnish families with Intellectual Disability - Four novel mutations and two novel syndromic phenotypes. *Orphanet J Rare Dis*. 2014;9(1):49. doi:10.1186/1750-1172-9-49

28. Martin S, Chamberlin A, Shinde DN, et al. De Novo Variants in GRIA4 Lead to Intellectual Disability with or without Seizures and Gait Abnormalities. *Am J Hum Genet*. 2017;101(6):1013-1020. doi:10.1016/j.ajhg.2017.11.004

29. Davies B, Brown LA, Cais O, et al. A point mutation in the ion conduction pore of AMPA receptor GRIA3 causes dramatically perturbed sleep patterns as well as intellectual disability. *Hum Mol Genet*. 2017;26(20):3869-3882. doi:10.1093/hmg/ddx270

30. Wu Y, Arai AC, Rumbaugh G, et al. Mutations in ionotropic AMPA receptor 3 alter channel properties and are associated with moderate cognitive impairment in humans. *Proc Natl Acad Sci U S A*. 2007;104(46):18163-18168. doi:10.1073/pnas.0708699104

31. Chérot E, Keren B, Dubourg C, et al. Using medical exome sequencing to identify the causes of neurodevelopmental disorders: Experience of 2 clinical units and 216 patients. *Clin Genet*. 2018;93(3):567-576. doi:10.1111/cge.13102

32. Hamanaka K, Miyoshi K, Sun JH, et al. Amelioration of a neurodevelopmental disorder by carbamazepine in a case having a gain-of-function GRIA3 variant. *Hum Genet*. Published online January 15, 2022. doi:10.1007/s00439-021-02416-7

33. Rinaldi B, Ge YH, Freri E, et al. Myoclonic status epilepticus and cerebellar hypoplasia associated with a novel variant in the GRIA3 gene. *neurogenetics*. Published online November 3, 2021. doi:10.1007/s10048-021-00666-1

34. Sun JH, Chen J, Ayala Valenzuela FE, et al. X-linked neonatal-onset epileptic encephalopathy associated with a gain-of-function variant p.R660T in GRIA3. zhang wei, ed. *PLOS Genet*. 2021;17(6):e1009608. doi:10.1371/journal.pgen.1009608

35. Martinez-Esteve Melnikova A, Pijuan J, Aparicio J, et al. The p.Glu787Lys variant in the GRIA3 gene causes developmental and epileptic encephalopathy mimicking structural epilepsy in a female patient. *Eur J Med Genet*. 2022;65(3):104442. doi:10.1016/j.ejmg.2022.104442

36. Philippe A, Malan V, Jacquemont ML, et al. Xq25 duplications encompassing GRIA 3 and STAG 2 genes in two families convey recognizable X-linked intellectual disability with distinctive facial appearance. *Am J Med Genet A*. 2013;161(6):1370-1375. doi:10.1002/ajmg.a.35307

37. Chiyonobu T, Hayashi S, Kobayashi K, et al. Partial tandem duplication of GRIA3 in a male with mental retardation. *Am J Med Genet A*. 2007;143(13):1448-1455. doi:10.1002/ajmg.a.31798

38. Allen NM, Conroy J, Shahwan A, et al. Unexplained early onset epileptic encephalopathy: Exome screening and phenotype expansion. *Epilepsia*. 2016;57(1):e12-e17. doi:10.1111/epi.13250

39. Jacquemont ML, Sanlaville D, Redon R, et al. Array-based comparative genomic hybridisation identifies high frequency of cryptic chromosomal rearrangements in patients with syndromic autism spectrum disorders. *J Med Genet*. 2006;43(11):843-849. doi:10.1136/jmg.2006.043166

40. Guilmatre A, Dubourg C, Mosca AL, et al. Recurrent rearrangements in synaptic and neurodevelopmental genes and shared biologic pathways in schizophrenia, autism, and mental retardation. *Arch Gen Psychiatry*. 2009;66(9):947-956. doi:10.1001/archgenpsychiatry.2009.80

41. Bonnet C, Leheup B, Béri M, Philippe C, Grégoire MJ, Jonveaux P. Aberrant GRIA3 transcripts with multi-exon duplications in a family with X-linked mental retardation. *Am J Med Genet A*. 2009;149(6):1280-1289. doi:10.1002/ajmg.a.32858

42. Yang Y, Muzny DM, Xia F, et al. Molecular findings among patients referred for clinical whole-exome sequencing. *JAMA*. 2014;312(18):1870-1879. doi:10.1001/jama.2014.14601

43. Hu H, Haas SA, Chelly J, et al. X-exome sequencing of 405 unresolved families identifies seven novel intellectual disability genes. *Mol Psychiatry*. 2016;21(1):133-148. doi:10.1038/mp.2014.193

44. LaDuca H, Farwell KD, Vuong H, et al. Exome sequencing covers >98% of mutations identified on targeted next generation sequencing panels. *PloS One*. 2017;12(2):e0170843. doi:10.1371/journal.pone.0170843

45. Hesse AN, Bevilacqua J, Shankar K, Reddi HV. Retrospective genotype-phenotype analysis in a 305 patient cohort referred for testing of a targeted epilepsy panel. *Epilepsy Res*. 2018;144:53-61. doi:10.1016/j.eplepsyres.2018.05.004

46. Lyu Y, Yang Y, Liu Y, Gai Z. Analysis of a patient with X-linked mental retardation by next generation sequencing. *Zhonghua Yi Xue Yi Chuan Xue Za Zhi Zhonghua Yixue Yichuanxue Zazhi Chin J Med Genet*. 2018;35(2):257-260. doi:10.3760/cma.j.issn.1003-9406.2018.02.025

47. Bai Z, Kong X. X-linked mental retardation combined with autism caused by a novel hemizygous mutation of GRIA3 gene. *Zhonghua Yi Xue Yi Chuan Xue Za Zhi Zhonghua Yixue Yichuanxue Zazhi Chin J Med Genet*. 2019;36(8):829-833. doi:10.3760/cma.j.issn.1003-9406.2019.08.019

48. Carraro M, Monzon AM, Chiricosta L, et al. Assessment of patient clinical descriptions and pathogenic variants from gene panel sequences in the CAGI-5 intellectual disability challenge. *Hum Mutat*. 2019;40(9):1330-1345. doi:10.1002/humu.23823

49. Fernández-Marmiesse A, Roca I, Díaz-Flores F, et al. Rare Variants in 48 Genes Account for 42% of Cases of Epilepsy With or Without Neurodevelopmental Delay in 246 Pediatric Patients. *Front Neurosci*. 2019;13. Accessed March 6, 2022. https://www.frontiersin.org/article/10.3389/fnins.2019.01135

50. Poot M, Eleveld MJ, van 't Slot R, Ploos van Amstel HK, Hochstenbach R. Recurrent copy number changes in mentally retarded children harbour genes involved in cellular localization and the glutamate receptor complex. *Eur J Hum Genet EJHG*. 2010;18(1):39-46. doi:10.1038/ejhg.2009.120

51. Alkelai A, Shohat S, Greenbaum L, et al. Expansion of the GRIA2 phenotypic representation: a novel de novo loss of function mutation in a case with childhood onset schizophrenia. *J Hum Genet*. 2021;66(3):339-343. doi:10.1038/s10038-020-00846-1

52. Latsko MS, Koboldt DC, Franklin SJ, et al. De novo missense mutation in GRIA2 in a patient with global developmental delay, autism spectrum disorder, and epileptic encephalopathy. *Cold Spring Harb Mol Case Stud*. 2022;8(4):a006172, mcs.a006172. doi:10.1101/mcs.a006172

53. Vijayaraghavan A, Urulangodi M, Ajit Valaparambil K, Sundaram S, Krishnan S. Movement Disorders in GRIA2-Related Disorder - Expanding the Genetic Spectrum of Developmental Dyskinetic Encephalopathy. *Mov Disord Clin Pract*. 2023;10(8):1222-1224. doi:10.1002/mdc3.13797

54. Cai Q, Zhou Z, Luo R, et al. Novel GRIA2 variant in a patient with atypical autism spectrum disorder and psychiatric symptoms: a case report. *BMC Pediatr*. 2022;22(1):629. doi:10.1186/s12887-022-03702-7

55. Okano S, Makita Y, Miyamoto A, et al. GRIA3 p.Met661Thr variant in a female with developmental epileptic encephalopathy. *Hum Genome Var*. 2023;10(1):1-4. doi:10.1038/s41439-023-00232-1

56. Wang H, Liu J, Li F, Teng Z, Liu M, Gu W. Novel Heterozygous Missense Variant in GRIA4 Gene Associated With Neurodevelopmental Disorder With or Without Seizures and Gait Abnormalities. *Front Genet*. 2022;13:859140. doi:10.3389/fgene.2022.859140

57. Ismail V, Zachariassen LG, Godwin A, et al. Identification and functional evaluation of GRIA1 missense and truncation variants in individuals with ID: An emerging neurodevelopmental syndrome. *Am J Hum Genet*. 2022;109(7):1217-1241. doi:10.1016/j.ajhg.2022.05.009

58. Firth HV, Richards SM, Bevan AP, et al. DECIPHER: Database of Chromosomal Imbalance and Phenotype in Humans Using Ensembl Resources. *Am J Hum Genet*. 2009;84(4):524-533. doi:10.1016/j.ajhg.2009.03.010

59. Landrum MJ, Lee JM, Benson M, et al. ClinVar: improving access to variant interpretations and supporting evidence. *Nucleic Acids Res*. 2018;46(D1):D1062-D1067. doi:10.1093/nar/gkx1153

60. Sobreira N, Schiettecatte F, Valle D, Hamosh A. GeneMatcher: a matching tool for connecting investigators with an interest in the same gene. *Hum Mutat*. 2015;36(10):928-930. doi:10.1002/humu.22844

61. Peng SX, Pei J, Rinaldi B, et al. Dysfunction of AMPA receptor GluA3 is associated with aggressive behavior in human. *Mol Psychiatry*. 2022;27(10):4092-4102. doi:10.1038/s41380-022-01659-8

62. Kiskin NI, Krishtal OA, Tsyndrenko AYa null. Excitatory amino acid receptors in hippocampal neurons: kainate fails to desensitize them. *Neurosci Lett*. 1986;63(3):225-230. doi:10.1016/0304-3940(86)90360-5

63. Otis T, Zhang S, Trussell LO. Direct measurement of AMPA receptor desensitization induced by glutamatergic synaptic transmission. *J Neurosci Off J Soc Neurosci*. 1996;16(23):7496-7504. doi:10.1523/JNEUROSCI.16-23-07496.1996

64. Hansen KB, Wollmuth LP, Bowie D, et al. Structure, Function, and Pharmacology of Glutamate Receptor Ion Channels. *Pharmacol Rev*. 2021;73(4):298-487. doi:10.1124/pharmrev.120.000131

65. Stern-Bach Y, Russo S, Neuman M, Rosenmund C. A point mutation in the glutamate binding site blocks desensitization of AMPA receptors. *Neuron*. 1998;21(4):907-918. doi:10.1016/s0896-6273(00)80605-4

66. Suzuki E, Kessler M, Arai AC. The fast kinetics of AMPA GluR3 receptors is selectively modulated by the TARPs gamma 4 and gamma 8. *Mol Cell Neurosci*. 2008;38(1):117-123. doi:10.1016/j.mcn.2008.01.018

67. Pei W, Huang Z, Niu L. GluR3 flip and flop: Differences in channel opening kinetics. *Biochemistry*. 2007;46(7):2027-2036. doi:10.1021/bi062213s

68. Magazanik LG, Buldakova SL, Samoilova MV, Gmiro VE, Mellor IR, Usherwood PNR. Block of open channels of recombinant AMPA receptors and native AMPA/kainate receptors by Adamantane derivatives. *J Physiol*. 1997;505(3):655-663. doi:10.1111/j.1469-7793.1997.655ba.x

69. Hampson DR, Manalo JL. The activation of glutamate receptors by kainic acid and domoic acid. *Nat Toxins*. 1998;6(3-4):153-158. doi:10.1002/(sici)1522-7189(199805/08)6:3/4<153::aid-nt16>3.0.co;2-1

70. Tsubokawa H, Oguro K, Masuzawa T, Nakaima T, Kawai N. Effects of a spider toxin and its analogue on glutamate-activated currents in the hippocampal CA1 neuron after ischemia. *J Neurophysiol*. 1995;74(1):218-225. doi:10.1152/jn.1995.74.1.218

71. Koike M, Iino M, Ozawa S. Blocking effect of 1-naphthyl acetyl spermine on Ca(2+)-permeable AMPA receptors in cultured rat hippocampal neurons. *Neurosci Res*. 1997;29(1):27-36. doi:10.1016/s0168-0102(97)00067-9

72. Twomey EC, Yelshanskaya MV, Vassilevski AA, Sobolevsky AI. Mechanisms of Channel Block in Calcium-Permeable AMPA Receptors. *Neuron*. 2018;99(5):956-968.e4. doi:10.1016/j.neuron.2018.07.027

73. Traynelis J, Silk M, Wang Q, et al. Optimizing genomic medicine in epilepsy through a gene-customized approach to missense variant interpretation. *Genome Res*. 2017;27(10):1715-1729. doi:10.1101/gr.226589.117

74. Zhao Y, Chen S, Swensen AC, Qian WJ, Gouaux E. Architecture and subunit arrangement of native AMPA receptors elucidated by cryo-EM. *Science*. 2019;364(6438):355-362. doi:10.1126/science.aaw8250

75. Schwenk J, Harmel N, Brechet A, et al. High-resolution proteomics unravel architecture and molecular diversity of native AMPA receptor complexes. *Neuron*. 2012;74(4):621-633. doi:10.1016/j.neuron.2012.03.034

76. van der Spek SJF, Pandya NJ, Koopmans F, et al. Expression and Interaction Proteomics of GluA1- and GluA3-Subunit-Containing AMPARs Reveal Distinct Protein Composition. *Cells*. 2022;11(22):3648. doi:10.3390/cells11223648

77. Wenthold RJ, Petralia RS, Blahos J, Niedzielski AS. Evidence for multiple AMPA receptor complexes in hippocampal CA1/CA2 neurons. *J Neurosci*. 1996;16(6):1982-1989. doi:10.1523/jneurosci.16-06-01982.1996

78. Sommer B, Keinänen K, Verdoorn TA, et al. Flip and flop: A cell-specific functional switch in glutamate-operated channels of the CNS. *Science*. 1990;249(4976):1580-1585. doi:10.1126/science.1699275

79. Monyer H, Seeburg PH, Wisden W. Glutamate-operated channels: developmentally early and mature forms arise by alternative splicing. *Neuron*. 1991;6(5):799-810. doi:10.1016/0896-6273(91)90176-z

80. Strehlow V, Heyne HO, Vlaskamp DRM, et al. GRIN2A-related disorders: genotype and functional consequence predict phenotype. *Brain J Neurol*. 2019;142(1):80-92. doi:10.1093/brain/awy304

81. Wolff M, Johannesen KM, Hedrich UBS, et al. Genetic and phenotypic heterogeneity suggest therapeutic implications in SCN2A-related disorders. *Brain J Neurol*. 2017;140(5):1316-1336. doi:10.1093/brain/awx054

82. Brunklaus A, Du J, Steckler F, et al. Biological concepts in human sodium channel epilepsies and their relevance in clinical practice. *Epilepsia*. 2020;61(3):387-399. doi:10.1111/epi.16438

83. Brunklaus A, Schorge S, Smith AD, et al. SCN1A variants from bench to bedside-improved clinical prediction from functional characterization. *Hum Mutat*. 2020;41(2):363-374. doi:10.1002/humu.23943

84. Masnada S, Hedrich UBS, Gardella E, et al. Clinical spectrum and genotype-phenotype associations of KCNA2-related encephalopathies. *Brain J Neurol*. 2017;140(9):2337-2354. doi:10.1093/brain/awx184

85. Johannesen KM, Liu Y, Koko M, et al. Genotype-phenotype correlations in SCN8A-related disorders reveal prognostic and therapeutic implications. *Brain J Neurol*. 2022;145(9):2991-3009. doi:10.1093/brain/awab321

86. Malerba F, Alberini G, Balagura G, et al. Genotype-phenotype correlations in patients with de novo KCNQ2 pathogenic variants. *Neurol Genet*. 2020;6(6):e528. doi:10.1212/NXG.0000000000000528

87. Benke TA, Park K, Krey I, et al. Clinical and therapeutic significance of genetic variation in the GRIN gene family encoding NMDARs. *Neuropharmacology*. 2021;199:108805. doi:10.1016/j.neuropharm.2021.108805

88. Han W, Yuan H, Allen JP, et al. Opportunities for Precision Treatment of GRIN2A and GRIN2B Gain-of-Function Variants in Triheteromeric N-Methyl-D-Aspartate Receptors. *J Pharmacol Exp Ther*. 2022;381(1):54-66. doi:10.1124/jpet.121.001000

89. Absalom NL, Liao VWY, Johannesen KMH, et al. Gain-of-function and loss-of-function GABRB3 variants lead to distinct clinical phenotypes in patients with developmental and epileptic encephalopathies. *Nat Commun*. 2022;13:1822. doi:10.1038/s41467-022-29280-x

90. Migeon BR. X-linked diseases: susceptible females. *Genet Med Off J Am Coll Med Genet*. 2020;22(7):1156-1174. doi:10.1038/s41436-020-0779-4

91. Srivastava S, Love-Nichols JA, Dies KA, et al. Meta-analysis and multidisciplinary consensus statement: exome sequencing is a first-tier clinical diagnostic test for individuals

with neurodevelopmental disorders. *Genet Med*. 2019;21(11):2413-2421. doi:10.1038/s41436-019-0554-6

92. Krey I, Platzer K, Esterhuizen A, et al. Current practice in diagnostic genetic testing of the epilepsies. *Epileptic Disord Int Epilepsy J Videotape*. 2022;24(5):765-786. doi:10.1684/epd.2022.1448

93. Brünger T, Pérez-Palma E, Montanucci L, et al. Conserved patterns across ion channels correlate with variant pathogenicity and clinical phenotypes. *Brain J Neurol*. 2023;146(3):923-934. doi:10.1093/brain/awac305

94. Arai AC, Kessler M. Pharmacology of ampakine modulators: from AMPA receptors to synapses and behavior. *Curr Drug Targets*. 2007;8(5):583-602. doi:10.2174/138945007780618490

95. Goff DC, Lamberti JS, Leon AC, et al. A placebo-controlled add-on trial of the Ampakine, CX516, for cognitive deficits in schizophrenia. *Neuropsychopharmacol Off Publ Am Coll Neuropsychopharmacol*. 2008;33(3):465-472. doi:10.1038/sj.npp.1301444

96. Wesensten NJ, Reichardt RM, Balkin TJ. Ampakine (CX717) effects on performance and alertness during simulated night shift work. *Aviat Space Environ Med*. 2007;78(10):937-943. doi:10.3357/asem.2055.2007

97. Senin U, Abate G, Fieschi C, et al. Aniracetam (Ro 13-5057) in the treatment of senile dementia of Alzheimer type (SDAT): results of a placebo controlled multicentre clinical study. *Eur Neuropsychopharmacol J Eur Coll Neuropsychopharmacol*. 1991;1(4):511-517. doi:10.1016/0924-977x(91)90004-e

98. Olson ME, Eubanks LM, Janda KD. Chemical Interventions for the Opioid Crisis: Key Advances and Remaining Challenges. *J Am Chem Soc*. 2019;141(5):1798-1806. doi:10.1021/jacs.8b09756

99. Lynch G, Gall CM. Ampakines and the threefold path to cognitive enhancement. *Trends Neurosci*. 2006;29(10):554-562. doi:10.1016/j.tins.2006.07.007

100. Yuan CL, Shi EY, Srinivasan J, Ptak CP, Oswald RE, Nowak LM. Modulation of AMPA Receptor Gating by the Anticonvulsant Drug, Perampanel. *ACS Med Chem Lett*. 2019;10(3):237-242. doi:10.1021/acsmedchemlett.8b00322

101. Potschka H, Trinka E. Perampanel: Does it have broad-spectrum potential? *Epilepsia*. 2019;60 Suppl 1:22-36. doi:10.1111/epi.14456

102. Coombs ID, Ziobro J, Krotov V, Surtees TL, Cull-Candy SG, Farrant M. A gain-of-function GRIA2 variant associated with neurodevelopmental delay and seizures: Functional characterization and targeted treatment. *Epilepsia*. 2022;63(12):e156-e163. doi:10.1111/epi.17419

103. Jackson AC, Nicoll RA. The expanding social network of ionotropic glutamate receptors: TARPs and other transmembrane auxiliary subunits. *Neuron*. 2011;70(2):178-199. doi:10.1016/j.neuron.2011.04.007

104. Schwenk J, Fakler B. Building of AMPA-type glutamate receptors in the endoplasmic reticulum and its implication for excitatory neurotransmission. *J Physiol*. 2021;599(10):2639-2653. doi:10.1113/JP279025

105. Silk M, Petrovski S, Ascher DB. MTR-Viewer: identifying regions within genes under purifying selection. *Nucleic Acids Res*. 2019;47(W1):W121-W126. doi:10.1093/nar/gkz457

Figure legends

Figure 1 Location of *GRIA3* variants in the GluA3 receptor and effect on glutamate-gated channel function. (A) Structural model of homomeric GluA3 receptor encoded by the *GRIA3* gene built from structures of the GluA2 receptor (*Supplementary materials & methods*). The top left panel shows a surface representation of the tetrameric receptor complex with the four identical subunits in shades of gray and blue. The bottom panel shows a cartoon representation of a single GluA3 subunit with the N-terminal domain (NTD) in light blue, the agonist-binding domain (ABD) in blue, and the transmembrane domain (TMD) in magenta. Zoomed views of the NTD, ABD, and TMD shows the position of genetic variants caused by *GRIA3* missense variants highlighted by different colors according to the apparent effect on homomeric GluA3 function as neutral (*gray*), LoF (*red*), and GoF (*green*). Orange circle indicate the position of the Glu binding site in the LBD. **(B)** Summary of desensitized (Glu) and non-desensitized (Glu+CTZ) current amplitudes and Glu EC50 for homomeric GluA3 receptors containing genetic variants encoded

by the *GRIA3* variants evaluated in this study. Values, number of measurements, and statistical parameters are given in Tables S2 and S3. Individual data points are color-coded according to the effect on currents or EC50 (LoF effect; *red*) or increase (GoF effect; *green*). For the EC50 panel, data points shown as squares represent EC50 values determined with CTZ. **(C)** Representative current responses from TEVC recordings of XO (V_{HOLD} -40 mV) expressing WT or *GRIA3* variant-containing GluA3 receptors in response to Glu application (300 µM, *black bar*) in the presence of CTZ (100 µM) to block desensitization. **(D)** Representative current recordings from TEVC Glu concentration-response experiments of WT GluA3 and selected variants exemplifying neutral (p.(Ala615Val)), increasing (p.(Ala654Val)), or decreasing (p.(Thr776Met)) effect on receptor responsiveness to Glu. **(E)** Composite concentration-response curves for WT and selected *GRIA3* variant-containing GluA3 receptors. Data points represent the mean of 6 to 12 oocytes. Error bars are the SEM and are shown when larger than the symbol size. The current responses are normalized to the maximal response evoked by Glu. In all panels, variants are labelled with single-letter amino acid codes.

Figure 2 Variant effects on receptor desensitization and activation properties. (A) Representative currents evoked by sequential 10-20 s applications of Glu (1 mM, *black bar*) alone and in the presence of CTZ (100 µM, *gray bar*) from oocytes expressing WT GluA3 and GluA3 carrying selected *GRIA3* missense variants. The p.(Pro302Ser) variant shows no change in the size of the desensitized current relative to the non-desensitized Glu current compared to WT, the p.(Ala654Val) variant shows increased desensitized current, and the p.(Thr816Ile) variant show decreased desensitized current. **(B)** Representative currents evoked by sequential 10-20 s applications of Glu (1 mM, black bar) and KA (300 µM; *blue bars*) in the presence of CTZ (100 µM, gray bar) from oocytes expressing WT GluA3 and GluA3 containing selected variants exemplifying different types of variant effects on KA/GLU response ratio. For WT GluA3 and the p.(Pro302Ser) variant, the KA-evoked current has an amplitude of 16% of the Glu current amplitude. In contrast, the p.(Ala654Val) variant has a relative KA current of 41%, indicating an increase in activation properties, and p.(Ala653Thr) variant has decreased relative KA response amplitude of 3.5%, indicating decreased activation properties. The holding potential was -40 mV in all shown recordings. **(C)** Representative currents illustrating NASPM (1 µM, red bar) inhibition of Glu evoked currents for WT GluA3 and GluA3 containing the

variants p.(Arg631Ser) and p.(Ala654Pro) **(D)** Summary of the ratio of desensitized and non-desensitized current amplitude ($I_{GLU}/I_{GLU+CTZ}$), non-desensitized Glu and KA ($I_{KA+CTZ}/I_{GLU+CTZ}$) current amplitudes and NASPM inhibition of Glu-evoked current for homomeric GluA3 receptors containing genetic variants encoded by the *GRIA3* variants evaluated in this study. Values, number of measurements, and statistical parameters are given in Table S2. Individual data points are color-coded according to the effect on currents or EC_{50} (LoF effect; *red*) or increase (GoF effect; *green*). **(E-G)** Summary of phenotype and domain location of variants with overall GoF (E), LoF (F), and neutral (G) effect on homomeric GluA3 receptor function. Symbols indicate: ▼; decrease, ▲; increase, ●; no change, -; not determined. Color coding indicates a predicted LoF (*red*) or GoF (*green*) effect of change on overall receptor function. **(H)** Missense tolerance ratio (MTR) of *GRIA3* variants analyzed with a 31 amino acid window calculated using the MTR-viewer online tool (https://biosig.lab.uq.edu.au/mtr-viewer/)[105]. A line graph displays the MTR distribution for *GRIA3* (gene transcript NM_000828) with regions in orange indicating observed variation differs significantly from neutrality. Dashed lines on the plot denote gene-specific MTRs: green = 5th percentile, purple = 25th percentile and black = 50th percentile. Above the MTR distribution is shown the domain structure of the GluA3 subunit. Variant positions are shown as circles on the MTR line graph and colored according to functional effect as: neutral (*gray*), GoF (*green*), and LoF (*red*). Orange line segments indicate regions where the observed variation differs significantly from neutrality. In all panels, variants are labelled with single-letter amino acid codes.

Figure 3 Variant effects in heteromeric GluA2/A3 receptors. (A) Representative currents evoked by sequential 10-20 s applications of Glu (1 mM, *black bar*) alone and in the presence of CTZ (100 µM, *gray bar*) from oocytes expressing WT GluA2 and WT GluA3 and WT GluA2 with GluA3 carrying selected *GRIA3* missense variants illustrating increased (p.(Ala654Val), *middle trace*) and decreased (p.(Leu774Ser); *lower trace*) desensitized current. **(B)** Representative currents evoked by sequential 10-20 s applications of Glu (1 mM, black bar) and KA (300 µM; *blue bars*) the presence of CTZ (100 µM, *gray bar*) from oocytes expressing WT GluA2 and WT GluA3 and WT GluA2 with GluA3 carrying selected *GRIA3* missense variants illustrating increased (p.(Ala615Val), *middle trace*) and decreased (p.(Ala653Thr); *lower trace*) current response to KA relative to Glu. **(C)** Representative current recordings from TEVC Glu

concentration-response experiments of WT and selected variants in heteromeric GluA2/A3 receptors with corresponding fitted dose-response curves for homomeric (A3) and heteromeric (A2/A3) receptors. The p.(Trp799Leu) exemplifies a variant changing the EC_{50} in both homomeric and heteromeric receptors, whereas p.(Thr776Met)) exemplifies a variant affecting only homomeric receptors. Color code of curves indicate effect on EC_{50}: Decrease (*green*), increase (*red*), or neutral (*gray*). **(D)** Overview and summary of the effects on heteromeric GluA2/A3 receptor parameters (*squares*) of *GRIA3* variants with GoF (*green*) and LoF (*red*) effects. Data points represent the mean and 95% CI values (see Supplementary Tables S2 and S3). **(E)** IV relationships of Glu-evoked currents from oocytes expressing homomeric WT and variant-containing GluA3 alone (*white circles*) and with WT GluA2R (*black circles*). The current amplitude at the different holding potentials is normalized to the current at -40 mV. Data points represent the mean from 6 to 10 oocytes. Error bars indicate the SEM and are shown when larger than the symbol size. In all panels, variants are labelled with single-letter amino acid codes.

Figure 4 Characterization of variant effect on fast receptor kinetics. **(A)** Representative whole-cell currents evoked by a 500 ms application of Glu (10 mM, *black bar*) from homomeric GluA3 (*left*) and heteromeric GluA2/A3 receptors carrying the indicated *GRIA3* variants subunits expressed in HEK293 cells. The holding potential was -70 mV in all recordings. Note that scale bars for current amplitude differ between recordings. **(B)** The time constant (τ_{des}) and level (I_{ss}) of current desensitization determined from the fitting of the current decay (*insert*) during 500 ms applications of Glu (10 mM, *black bars*) fitted to two-exponential decay functions weighted by proportional contributions for WT and variant homomeric GluA3 (*left*) and heteromeric GluA2/A3 (*right*) receptors. **(C)** Summary of the τ_{des} and I_{ss} values. Bars represent the mean with SEM error. Values not determined due to low or no current are labelled *nd*. **(D)** Deactivation rates (τ_{deact}) determined from the fitting of the current decay (*insert*) following 1 ms application of Glu (10 mM, *black bars*) fitted to a mono-exponential decay function (*inserts*) for WT and variant homomeric GluA3 (*left*) and heteromeric GluA2/A3 (*right*) receptors. **(E)** Summary of τ_{deact} values. Bars represent the mean with SEM error. Values not determined due to low or no current are labelled *nd*. **(F)** Summary of effects of patient variants on current kinetics and location in GluA3 subunit. Variants with LoF effects are shown in red and GoF in green. ▼;

decrease, ▲; increase, ●; no change, -; not determined. In all panels, variants are labelled with single-letter amino acid codes.

Figure 5 Variant classification and phenotype correlations for patient M1-M12 and F1-F10. **(A)** Schematic overview of the classification of receptor phenotype for patients M1-M13 and F1-F11 into severe and mild GoF (*green*) and LoF (*red*) categories based on variant effect patterns on GluA3-containing receptor function together with an overview of the number of patients and prevalence of key patient symptoms for each category. **(B)** Summary of key and supporting features for the clinical phenotypes associated with LoF and GoF variants. The diagram summarizes several clinical findings that can help predict if a *GRIA3* variant leads to loss-of-function (LoF) and gain-of-function (GoF). GoF variants manifest with seizures occurring before the first year of life (with a median age of 1 month) and are characterized by supporting features such as hypertonia, hyperekplexia/excessive startle reflex, and the absence of sleep disturbances. LoF variants manifest with key features such as seizure onset after the first year of life (with a median age of 16 months) and supporting features including hypotonia, sleep disturbances, and the absence of hyperekplexia/excessive startle reflex. If a patient's phenotypical presentation displays a combination of these features, functional testing of the variant is required to determine whether a *GRIA3* variant displays LoF or GoF characteristics. [a-d] *P* values for comparing proportions of clinical indicators between the LoF or GoF patients: [a] Age of seizure onset < 12 months versus age of seizure onset > 12 months; $P = 0.004$, [b] hypertonia versus hypotonia; $P = 0.0004$, [c] hyperekplexia/startle versus no hyperekplexia/startle; $P = 0.003$, [d] sleep disturbance versus no sleep disturbance; $P = 0.018$.

Table 1 Comparison of clinical features reported in patients with loss-of function *GRIA3* variants compared to features reported in those with gain-of-function *GRIA3* variants

Feature	Loss-of-function	Gain-of-function
Number of patients	15	10
Male	12/15 (80%)	2/10 (20%)
Female	3/15 (20%)	8/10 (80%)
Epilepsy diagnosis	5/15 (33%)	6/10 (60%)
Median age at onset of seizures	16 months (range 9 mo to 3 yrs)	1 month (range 1st day to 27 yrs)
Treatment resistant seizures	3/5 (60%)	4/6 (66%)
Developmental delay or cognitive impairment	15/15 (100%)	10/10 (100%)

	Degree: borderline = 1 mild-moderate= 1 moderate = 4 severe = 7 severe-profound = 1 profound = 1	Degree: moderate = 4 severe = 2 severe-profound = 1 profound = 3
Muscular hypotonia	12/15 (80%)	0/10 (0%)
Muscular hypertonia	2/15 (13%)	9/10 (90%)
Hyporeflexia	10/15 (66%)	0/10 (0%)
Hyperreflexes	1/15 (6%)	7/10 (70%)
Spasticity	1/15 (6%)	4/10 (40%)
Movement disorder or any kind	7/15 (46%)	8/10 (80%)
Hyperexplexia or stimulus sensitive non-epilepticus myoclonia	2/15 (13%)	6/10 (60%)
Sleep disorder	10/15 (66%)	3/10 (33%)
Behavioral issues of any kind	10/15 (66%)	5/10 (50%)
Aggressive outburst or self-damaging behavior	6/15 (40%)	2/10 (20%)
Magnetic resonance imagiging (MRI) performed	9/15 (60%)	9/10 (90%)
Abnormal MRI	2/9 (22%)	2/9 (22%)

The table summarizes key clinical features in the loss-of-function and gain-of-function patient groups. Detailed clinical information for individual patients is provided in Suplemtary Information and Table S7.

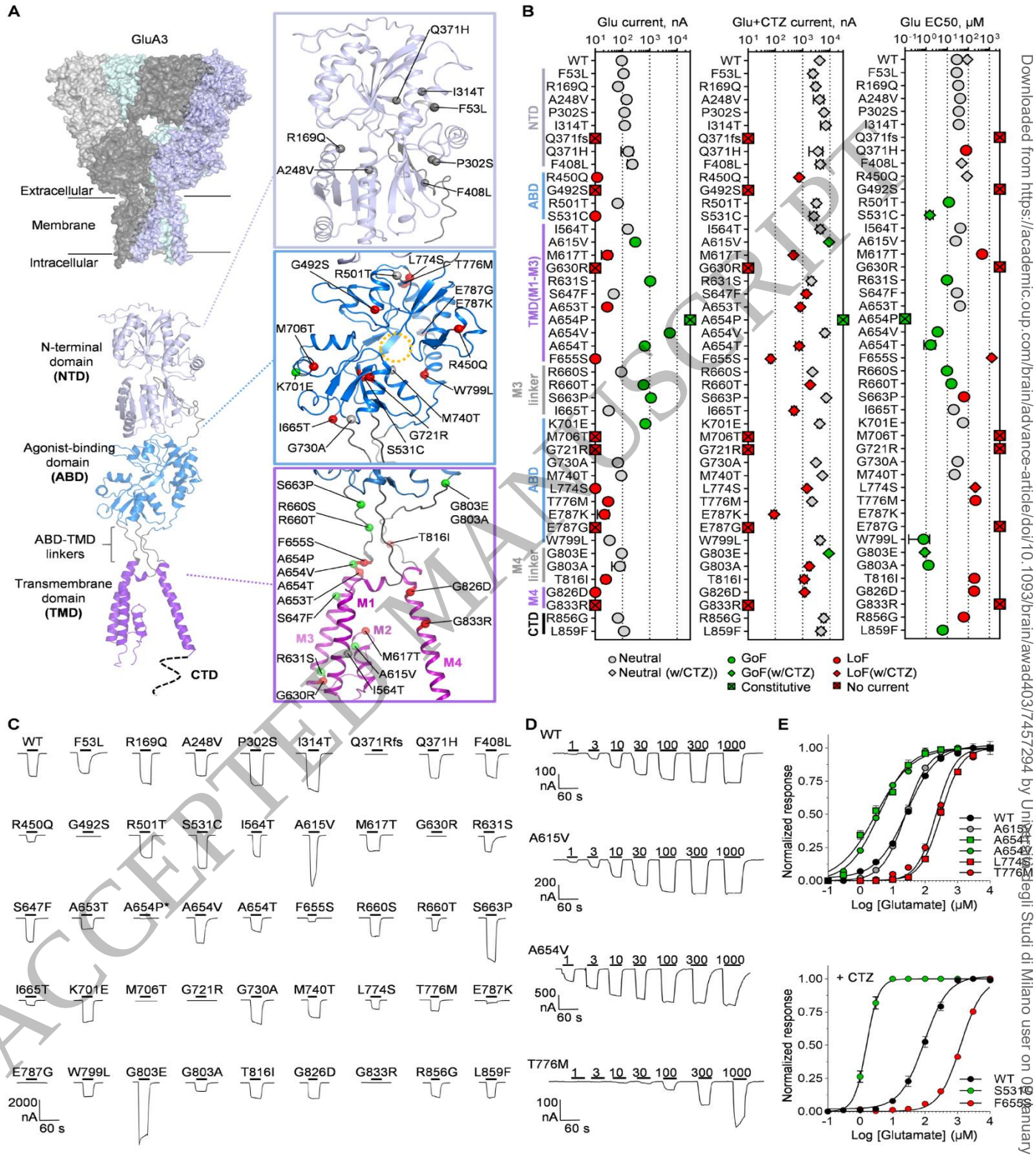

Figure 1

185x231 mm (x DPI)

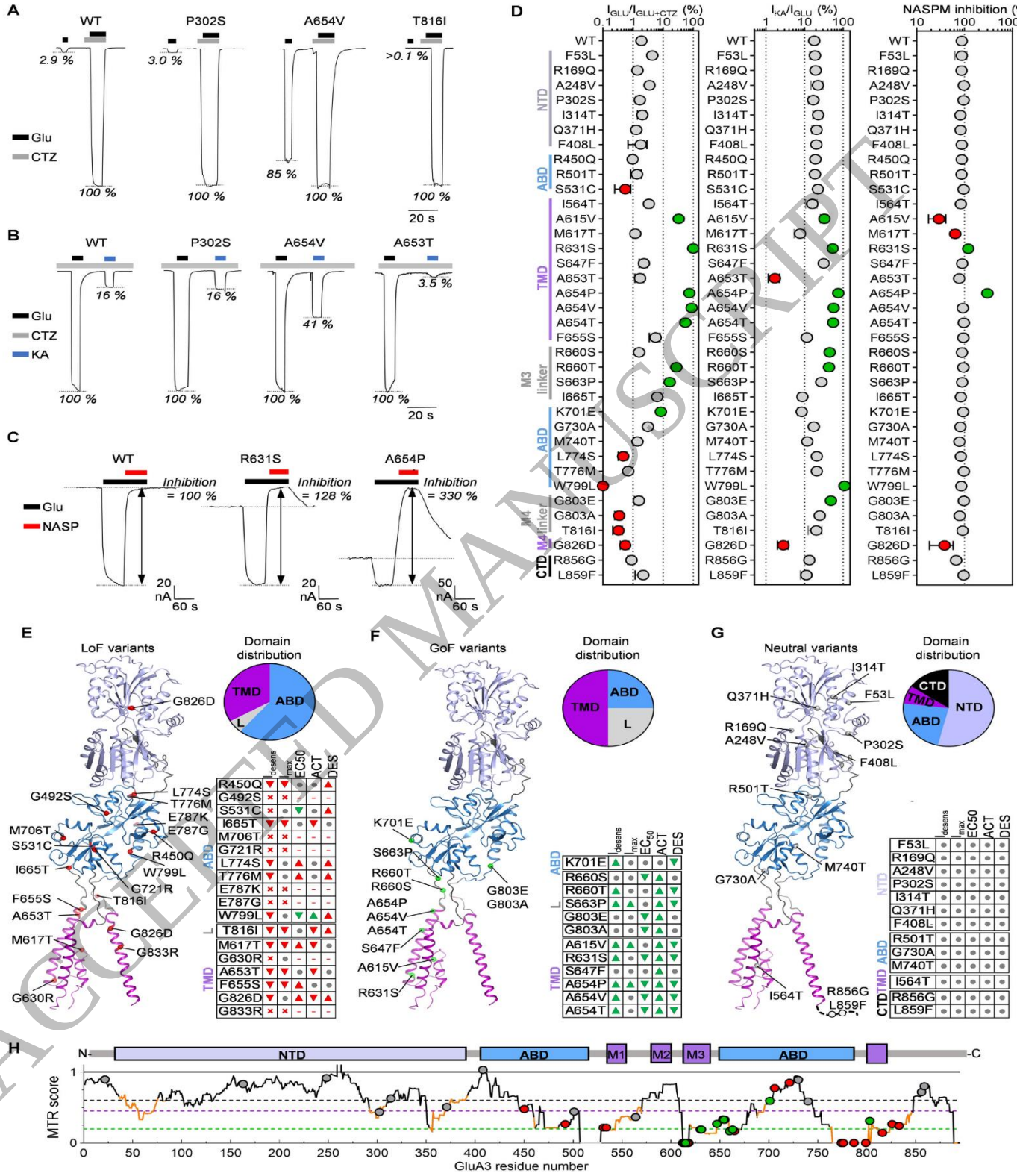

Figure 2

185x247 mm (x DPI)

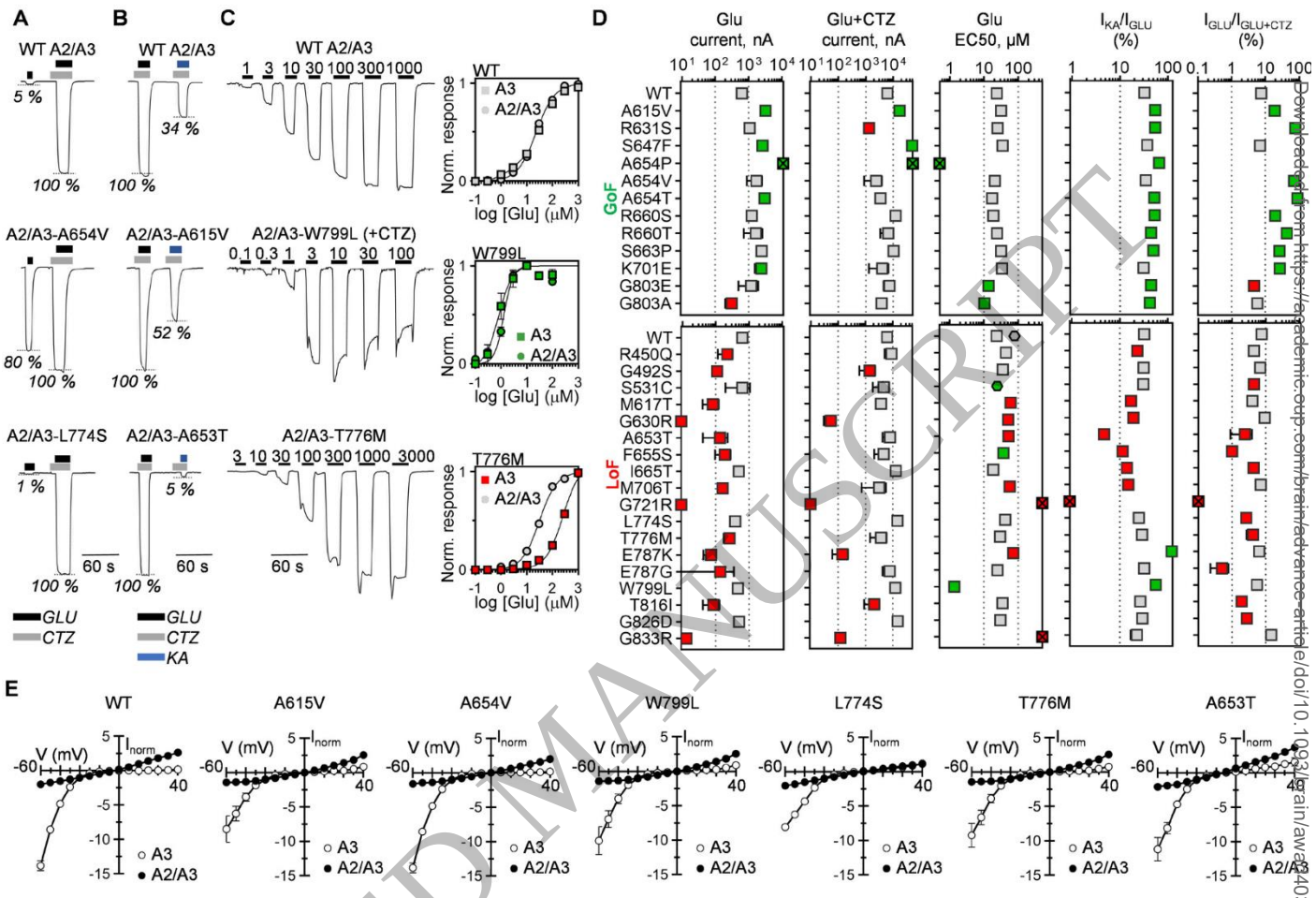

Figure 3
185x127 mm (x DPI)

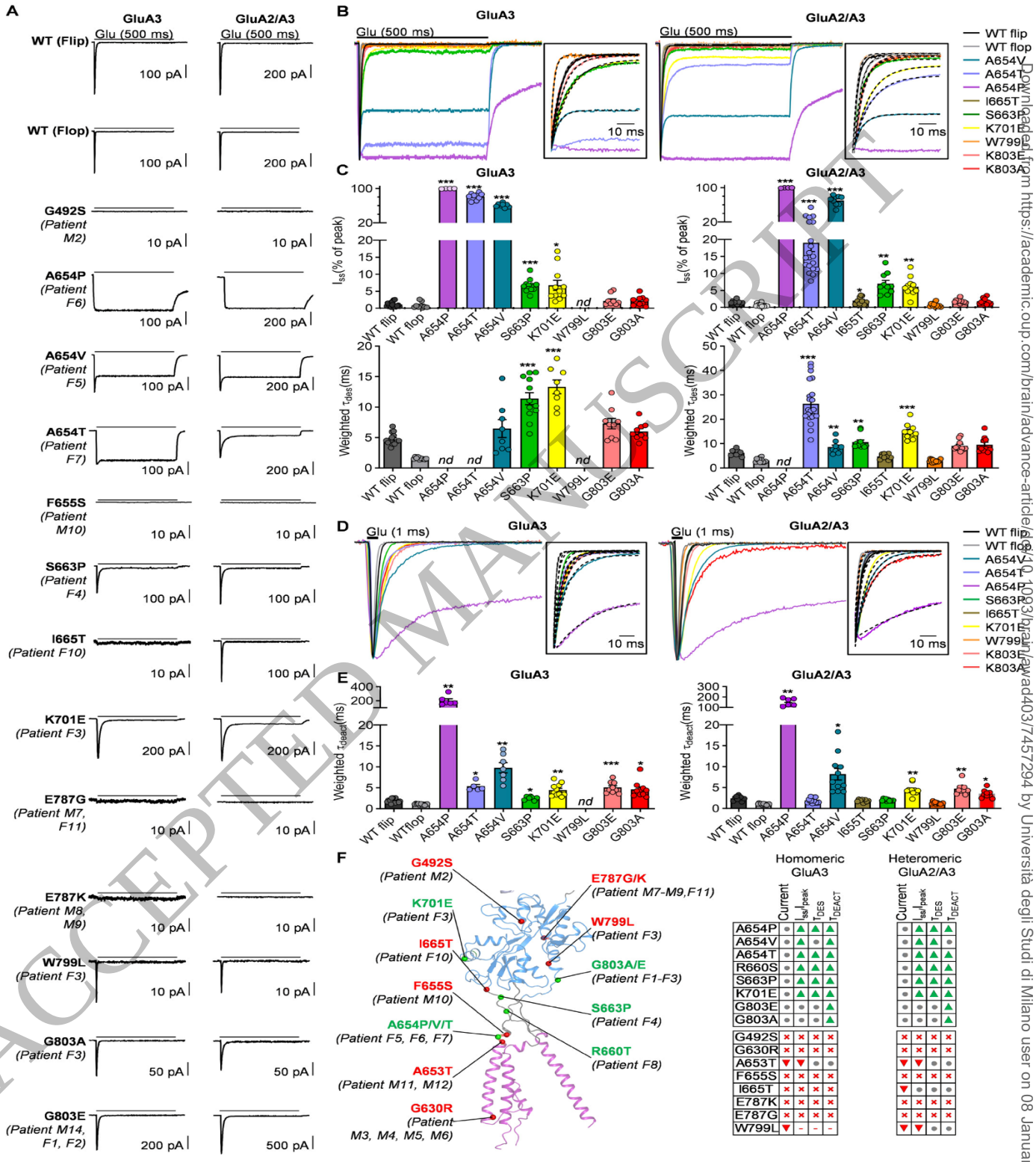

Figure 4

185x247 mm (x DPI)

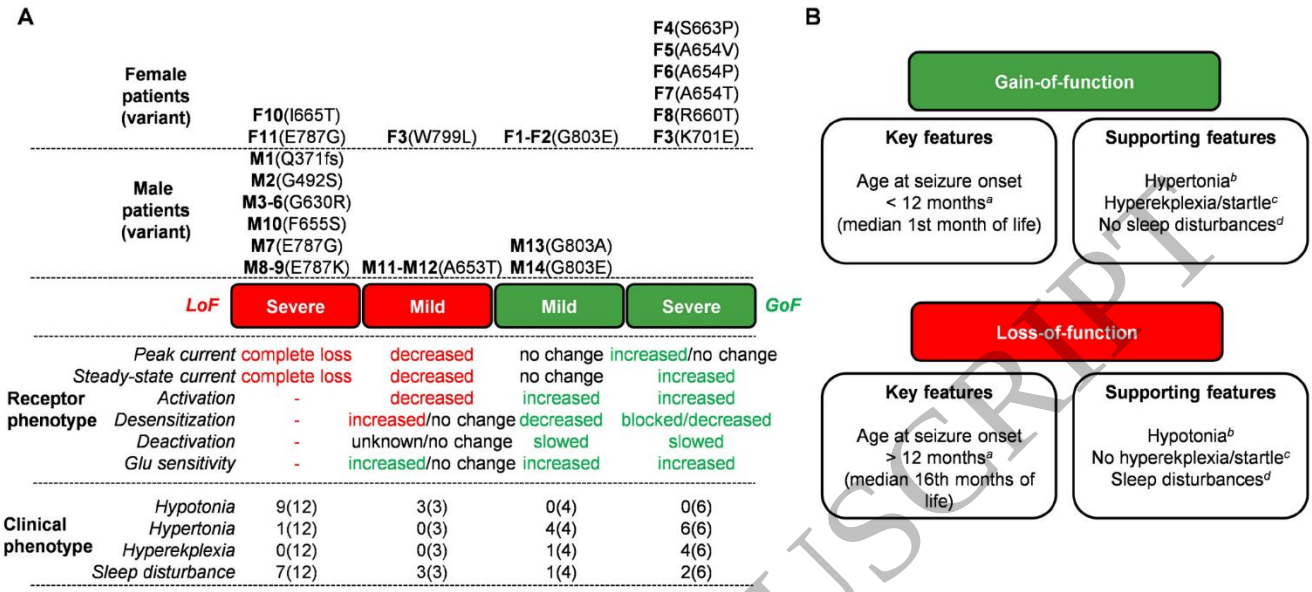

Figure 5
177x80 mm (x DPI)